WILEY | Hindawi

Research Article

Merging Sequence Optimization Based on Reverse Auction Theory and Merging Strategy with Active Trajectory Adjustment of Heterogeneous Vehicles

ShiHui Wang, Min Zhao [iD], DiHua Sun, and Xiaoyu Liu

School of Automation, Chongqing University and Key Laboratory of Dependable Service Computing in the Cyber Physical Society of the Ministry of Education, Chongqing University, Chongqing, China

Correspondence should be addressed to Min Zhao; zhaomin@cqu.edu.cn

This paper investigates the optimized merging sequence (MS) and on-ramp merging strategy in mixed traffic with vehicle-to-vehicle (V2V) and vehicle-to-infrastructure (V2I). To this end, a cooperative merging sequence optimization method is first proposed based on the reverse auction. In the method, a hybrid optimized computing structure is proposed to provide the foundation for connected and human-driving vehicles (CHVs) and connected and automated vehicles (CAVs) to obtain the MS more efficiently. And a cooperative merging strategy based on all cooperative merging vehicles under mixed traffic conditions is proposed. In particular, the downstream vehicles in the strategy can change their original velocities to actively participate in the cooperative merging process according to the merging requirements of on-ramp vehicles. And the vehicles in this strategy are all subject to state constraints to avoid the adverse effects of cooperative merging behavior on the following traffic on the main road. Results of numerical experiments illustrate that the merging sequence optimization method can reduce the time to obtain the optimal MS, and the increased computational efficiency is affected by CAV penetration. In addition, in mixed traffic conditions, the cooperative merging strategy can reduce fuel consumption and the time required for merging.

1. Introduction

As one of the classic bottleneck areas, traffic congestion often occurs in the on-ramp area, leading to a significant reduction in traffic efficiency [1]. Therefore, the merging of vehicles on ramps in the on-ramp area has been a hot topic of research in the traffic field [2]. Meanwhile, with the widespread application of communication and automation technology in the transportation field (eg., vehicle-to-vehicle (V2V) communications and vehicle-to-infrastructure (V2I) communications), CAVs have been receiving extensive attention because they can improve safety, reduce fuel consumption [3], relieve congestion [4], and increase passenger comfort [5]. It is foreseeable that all vehicles on the road in future intelligent transportation systems will be CAVs [6–8]. However, the full application of CAV in transportation currently still requires appropriate policies [8] and social trust [10]. At the same time, drivers of CHVs have access to more extensive and accurate traffic information through advanced communications for more effective vehicle control [11]. Therefore, it is certain that in the future, the two types of vehicles will coexist until CAVs completely replace CHVs. However, during this transitional period, mixed vehicles make the traffic situation in the on-ramp merging zone more complicated [12].

One of the purposes of this study is to enable CAVs and CHVs in the on-ramp area to obtain the optimal MS in a shorter computation time. From the perspective of global optimal coordination, Jing et al. [13] took fuel consumption, passenger comfort, and travel time as global pay-off conditions and then proposed an optimization structure and an algorithm to obtain the minimum value of the vehicle's global pay-off. Raravi et al. [14] represent the combined problem as a nonlinear optimization problem and obtain a locally optimal solution. To reduce the computational cost,

Li and Wang [15] and Awal et al. [16] all proposed a pruning algorithm to determine the merging sequence. Ding et al. [17] proposed a rule-based adjustment algorithm to obtain a near-optimal merge sequence and compared its results with optimality-based methods. Wang et al. [18] proposed a selection algorithm to determine the merging sequence based on the initial states of the vehicles in the cooperative area and obtained the optimal longitudinal trajectories of facilitating vehicle and on-ramp vehicle by solving the Hamiltonian function. Although the above studies have all proposed effective methods for obtaining the optimal MS, they consider scenarios where all vehicles are CAVs and do not consider the scenarios of mixed traffic.

As far as we know, the vast majority of studies still consider the scenarios of mixed traffic consisting of CAVs and conventional human-driving vehicles. Karimi et al. [19] outline a hierarchical control framework for on-ramp merging areas and designed a set of optimal trajectory control algorithms for CAV when mixed traffic is a mixture of CAVs and traditional human-driving vehicles, but the order of merging in this study is determined in advance. Ding et al. [20] proposed an integrated combined sequence scheduling strategy and motion planning method for the hierarchical cooperative merging of CAVs in mixed traffic, and their simulation experiment proved the performances (eg., throughput, delay, fuel consumption, and emission) of mixed traffic with the increase of CAV penetration were improved. [19]. Larsson et al. [21] proposed a prosocial control algorithm that considers driver comfort and traffic efficiency in order to alleviate to mitigate jamming waves in autonomous multilane traffic with a mixture of CAVs and human-driven vehicles. Experimental results show that prosocial control can provide higher efficiency and a more comfortable driving experience compared to personal driving. However, few of them consider the optimal MS in the mixed condition of CAVs and CHVs. Different from traditional human-driving vehicles, although CHVs still rely on driver operation, they can actively participate in the cooperative process by obtaining more effective traffic information and inducing information through V2I/V2V. In the V2I/V2V situation, while the on-ramp CHVs are safer driving to merge onto the main road, it also takes more time for drivers to complete the lane change, making the merging process more complicated [22]. Therefore, the merging of on-ramps for mixed CHV and CAV traffic in a V2I/V2V environment is very tricky. As the basis for the on-ramp vehicles to complete the merging, it is an important and challenging problem to make the coordinated CAV and CHV in the on-ramp area quickly obtain the optimal MS.

In addition, most of the current studies are based on a conventional merging strategy, which focuses on the co-operation of the main-road upstream vehicles and the on-ramp vehicles, while ignoring the role of vehicles in front of the target merging location. From the perspective of smooth traffic flow and avoiding stop-and-go driving, Rios-Torres and Malikopoulos [23] proposed a framework that allows online coordination of vehicles, which can significantly reduce fuel consumption and travel time. Zhou et al. [24] reduced the trajectory planning problem of the on-ramp

merging car and the mainline roller to two related optimal control problems and solved them by the Pontryagin principle of maximum. Based on this research, to prevent facilitating maneuvers from impacting traffic following them, Zhou et al. [25] also considered the state constraints of vehicles in the collaborative merging process and used the Pontryagin maximum principle with state constraints to strictly derive the analysis solution. Karbalaieali et al. [26] proposed a dynamic adaptive algorithm that does not require frequent deceleration or waiting for merging gaps at the end of the ramp and has minimal interference with mainline traffic, which ensures that the on-ramp connected automated vehicles can merge smoothly into the main-road platoon and improves the merging efficiency. Li et al. [27] proposed an intelligent connected vehicles active fine lane management method for the traffic congestion problem in the fusion zone. By controlling the intelligent connected vehicles to complete the lane change before reaching the weaving area, it ensures that the vehicles in the fusion zone complete the lane change within the specified time and reduces the traffic delay. Chai et al. [28] proposed a rein-forcement learning-based optimal entrance ramp control method that avoids the need to build an accurate traffic model and the reliance on a priori knowledge by iterating the value function with the actual behavior. To avoid vehicle collisions in the process of merging, Jing et al. [29] proposed a centralized collaborative vehicle trajectory planning structure for SAE level 4 or 5 automation, and a side friction collision prediction algorithm that takes into account the geometric characteristics of the vehicle. However, the co-operative merging methods in these studies have a potential assumption; that is, the velocities of main-road vehicles before the target merging location remain unchanged during the cooperative merging process. Although this assumption can simplify the research, it makes the vehicle before the target merging location can not be fully involved in the cooperative and does not match the actual traffic situation. At the same time, this assumption prevents cooperative vehicles from using downstream vehicles of the target merging position to save time and fuel consumption. Considering these issues, we have done work in the early stage [30]. However, our previous work did not consider the complex traffic environment of mixed CAV and CHV. Compared with previous work where all vehicles are considered to be CAVs, how to enable heterogeneous vehicles to accomplish merging collaboratively is one of the difficulties addressed by the merging strategy in this paper. And, the optimal sequence of cooperative merging in mixed traffic situations is not considered either. Therefore, the cooperative on-ramp merging strategy in mixed traffic is proposed, which can make full use of the cooperation of the vehicles in front of the target merging position to achieve a more efficient merge with less fuel consumption when CAVs and CHVs coexist.

The literature review and analysis heretofore illustrate that the challenges of cooperative merging in the on-ramp area mainly come from vehicle types and simplified research assumptions. Hence, this study seeks to design a novel MS optimization method that can be applied to mixed traffic

based on V2V and V2I, and a cooperative merging strategy that can make full use of all coordinated vehicles. The main contributions of this paper are threefold:

(1) In V2V and V2I environments, the idea of the reverse auction is introduced to design a novel MS optimization method for mixed traffic consisting of CHVs and CAVs. Different from the conventional centralized calculation method, the method is a hybrid calculation method for optimizing MS, in which CAV uses its onboard equipment and CHV uses roadside infrastructure to complete the calculations required to optimize MS. The proposed method can reduce the computation time needed to optimize MS, and the optimal MS obtained by this method can reduce the merging time and fuel consumption.

(2) Unlike the existing conventional cooperative merging strategies in which the downstream vehicle of the target merging position either does not directly participate in the cooperative merging process except for sharing its vehicle state information, this study makes the vehicles before the target merging location actively participate in the cooperative merging by adjusting their velocities so as to facilitate the merging. Further, state constraints on cooperative vehicles are applied in the strategy to reduce the negative impact of the merging on the main-lane traffic. This strategy can ensure collision-free merging while improving merging efficiency and reducing fuel consumption.

(3) The influence of CAV penetration on the MS optimization method proposed in this paper is investigated. With the increase in CAV penetration, the improved computation efficiency of this method is more obvious compared with the conventional centralized method.

The remainder of the paper is organized as follows. Section 2 analyzes the freeway cooperative merging from the cyberphysical system and then formulates the problem at the on-ramp. Section 3 presents an MS optimization method based on the reverse auction and the on-ramp merging strategy that the state of all cooperative vehicles are variable while considering merging behavior and its impact on the main-road traffic. Section 4 verifies the effectiveness and advantages of the proposed method and strategy through numerical simulation experiments and studies the influence of CAV penetration. Finally, some conclusions are outlined in Section 5.

2. Problem Description

In the future intelligent transportation, transportation will be a cyberphysical system [31]. In the system, this information such as pavement information, vehicle status, and location information is all collected by using perceptive equipment such as radar, as shown in Figure 1. In cyberspace, this information can be used to compute control orders, as shown in the cyberspace of Figure 1. At the same time, vehicles, drivers, and infrastructures can obtain information and control orders from cyberspace with a connected

network. In this paper, a typical directional on-ramp which is a single lane in each link is considered, as shown in the physical space of Figure 1, [32]. The blue vehicle, yellow vehicle, and black shaded area represent the CAV, CHV, and merging zone, respectively. And in the paper, the lane change behavior is not considered as presented in [25, 28, 29, 32].

Once the vehicle of the on-ramp arrives at the call for cooperation line (CCL), the definition of the MS which represents the sequence of driving into the merging zone is necessary. The most widely used method is FIFO. In the method, the MS of vehicles is determined based on the distance or time-till-arrival to the merging zone [16]. However, before moving into the merging zone, vehicles still can choose a different MS. In other words, which vehicle moves into the merging zone first does not necessarily need to be determined based on the distance or time-till-arrival to the merging zone. In other words, the on-ramp merging vehicles can be merged between any two vehicles on the main road. Taking the situation in Figure 1 as an example, we can find that there are three positions between main-road vehicles where the on-ramp vehicle can merge in, as shown in Figure 2. When the merging vehicle is ready to merge into different gaps, it means that the main-lane and on-ramp vehicles enter the merging zone in a different sequence. At this time, which sequence is beneficial to traffic is undoubtedly an optimization problem. At present, many of the research results on this issue are based on a centralized optimization structure, where all optimizations are calculated in one center for optimal MS [12–18]. This approach is not conducive to getting the optimal MS quickly. At the same time, Figure 2 also shows that different vehicle synergies are likely to result in different optimal MS. In many of the existing related studies, the cooperative merging is generally the main-road downstream vehicle to maintain the same velocities while the upstream cooperative vehicles adjust their state. Once the effects of cooperative merging on traffic are taken into account, the time required to complete merging will increase significantly. Therefore, the research focus of this paper is these two issues.

During the process, the dynamics of each vehicle can be modeled, as shown in [30], by the following nonlinear input-affine differential (1) which encompasses the engine dynamics, brake system, and aerodynamics drag.

$$\dot{a}(t) = f(v(t), a(t)) + g(v(t))c(t), \quad (1)$$

where $c(t)$ is the input to the engine of the vehicle and the nonlinear functions $f(v(t), a(t))$, and $g(v(t))$ are

$$f(v(t), a(t)) = -\frac{1}{\tau}\left(a(t) + \frac{\sigma\phi c_d}{2m}v(t) + \frac{d_m}{m}\right) - \frac{\sigma\phi c_d}{m}v(t)a(t),$$

$$g(v(t)) = \frac{1}{\tau m}, \quad (2)$$

where σ denotes the specific mass of the air, ϕ is the cross-sectional area, c_d is the drag coefficient, m denotes the mass of the vehicle, d_m represents the mechanical drag, and τ symbolizes the engine time constant (also called the inertial time-lag). The term $\sigma\phi c_d/2m$ is the model of air resistance.
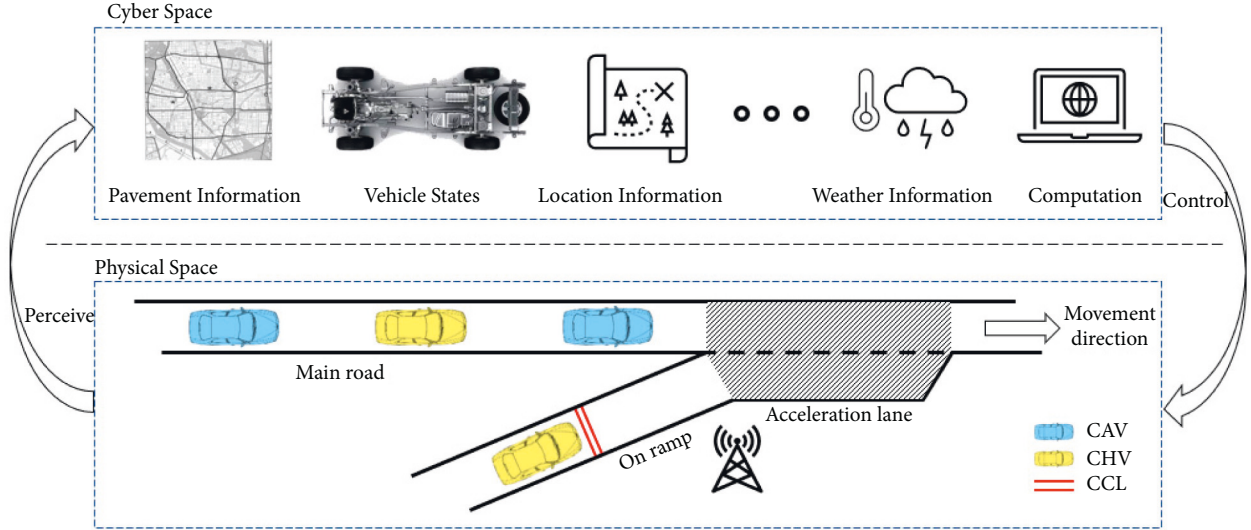
FIGURE 1: Cyberphysical systems in future intelligent transportation.
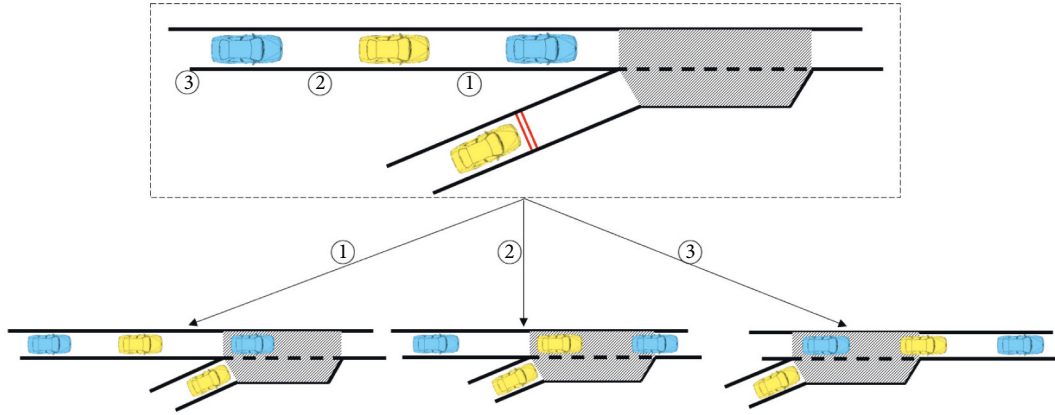

FIGURE 2: An example of the possible merging sequence.

To simplify the system model, we adopt the following feedback linearizing control law excluding some characteristic parameters of the vehicle from its dynamics.

$$c(t) = u(t)m + 0.5\sigma\phi c_d v(t) + d_m + \tau\sigma\phi c_d v(t)a(t), \quad (3)$$

where u is the additional input signal to be designed. Substituting (4) into (1), we can obtain the third-order dynamics model of the vehicle as

$$\begin{cases} \dot{p}(t) = v(t), \\ \dot{v}(t) = a(t), \\ \tau\dot{a}(t) + a(t) = u(t). \end{cases} \quad (4)$$

Then, we can get

$$\dot{x}(t) = Ax(t) + Bu(t), \quad (5)$$

where $A = \begin{bmatrix} 0 & 1 & 0 \\ 0 & 0 & 1 \\ 0 & 0 & -1/\tau \end{bmatrix}$, $B = \begin{bmatrix} 0 \\ 0 \\ 1/\tau \end{bmatrix}$, $x(t) = [p(t), v(t), a(t)]^T$, $p(t)$ is the position of the vehicle, $v(t)$ is the velocity of the vehicle, $a(t)$ is the acceleration, $u(t)$ is the control input, and

t is the time. t_0 represents the time when the on-ramp merging vehicle arrives at the CCL, and $x(t_0)$ is the initial state.

3. Methodology

In this section, we first propose a merging sequence optimization method based on reverse auction theory and then consider the negative effect of merging on main-road traffic and taking full advantage of all vehicles. The framework composed of the methods is shown in Figure 3.

The left side of the framework is the merging sequence optimization method, and the right side is the on-ramp merging strategy. The purpose of the merging sequence optimization method is to find the optimal merging sequence among many possible merging sequences to achieve some specific goals, such as ensuring safety, improving efficiency, and reducing fuel consumption. On-ramp cooperative merging strategy is to avoid conflicts between vehicles and obtain vehicles' trajectory or state under a given merging sequence. From this framework diagram, we can clearly know
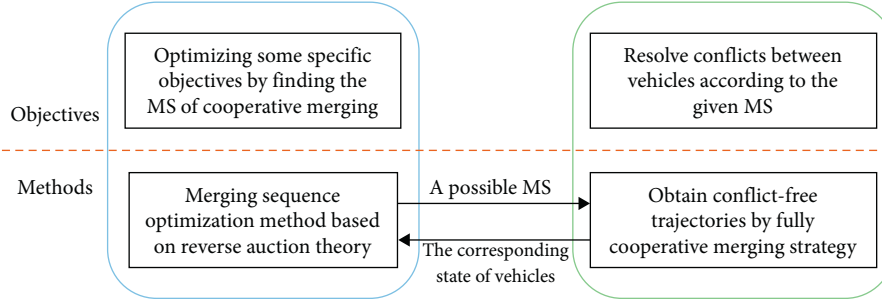
FIGURE 3: A framework constructed by the methods.

the connection between the merging sequence optimization method and the on-ramp merging strategy. In the framework, the merging sequence optimization method on the left part passes a possible merging sequence to the on-ramp merging strategy on the right part. After receiving the MS, the fully cooperative merging strategy obtains trajectories or state of vehicles under this MS through a series of calculations and returns this information to the merging sequence optimization method. Finally, after obtaining the trajectories or state of vehicles in all possible MS situations, the merging sequence optimization method based on reverse auction theory determines the optimal MS through specific calculation. Next, we introduce the merging sequence optimization method and merging strategy in detail.

3.1. A Merging Sequence Optimization Method Based on Reverse Auction Theory. Auction is an ancient trading method, which is widely used in all kinds of resource optimization. From the creation of modern auction theory by William Vickery in 1961 to the Nobel Prize in Economics for Paul R. Milgrom and Robert B. Wilson in 2020, auction theory has made considerable progress in basic research and application [33–35]. In an auction, all participants need to be able to make independent bids or purchases. At present, the types of auctions can be divided into Dutch auction, British auction, sealed auction, and reverse auction [36, 37]. In these forms, the reverse auction refers to the situation of one buyer and multiple sellers. In this form of auction, multiple sellers compete with each other to serve the buyer at the lowest price. In this paper, we look at each vehicle on the main road as a seller and the vehicle on the ramp seeking the merging position as a buyer. During the determine MS phase, each main-road vehicle is required to provide a quote to the on-ramp vehicle preparing to merge into the mainline behind it. Under the mechanism of independent offers from sellers in the reverse auction, the vehicle needs to bear the calculations required to give the offer. This distributed calculation will undoubtedly reduce the time to obtain MS and increase the efficiency of obtaining MS.

ptHowever, CHV only has simple communication capabilities and cannot accurately process traffic information without an onboard computer during the cooperative merging process. Considering that the vehicle

needs to be able to bid or purchases independently and to ensure that CHV can participate in the auction when acquiring MS through the reverse auction method, we design a novel hybrid calculation structure in the V2V/I environment of mixed traffic, as shown in Figure 4(b). The proposed structure is a mixture of centralized and distributed computing architecture. In this hybrid computing architecture, we have tried to introduce the idea and method of the reverse auction in order to acquire MS efficiently.

In this structure, all CHVs adopt a centralized calculation architecture, relying on infrastructure to perform the computation. All CAVs adopt a distributed architecture and rely on their own onboard computers. Unlike the structure used in many of the current studies shown in Figure 4(a) [12, 16], the vehicles in the structure we are talking about are involved in optimizing MS calculations to disperse computational loads, not just collecting and receiving information.

We consider the main-lane vehicles $j \in \{1, 2, \ldots, m\}$ as the sellers $s_j \in \{s_1, s_2, \ldots, s_m\}$, the on-ramp merging vehicle $i \in \{1', 2', \ldots, n'\}$ when arriving at CCL as the buyer $b_i \in \{b_{1'}, b_{2'}, \ldots, b_{n'}\}$, and the potential target merging location of vehicle i as the commodities $g_i = \{g_{i1}, g_{i2}, \ldots, g_{im}\}$. Each seller s_j puts a price $\text{bid}_i = \{\text{bid}_i^{g_{i1}}, \text{bid}_i^{g_{i2}}, \ldots \text{bid}_i^{g_{im}}\}$ on their corresponding goods.

We stipulate that the price $\text{bid}_i^{g_{ij}}$ of seller s_j is given according to

$$\text{bid}_i^{g_{ij}} = \omega_1 f_{\text{totalT}}^{g_{ij}} + \omega_2 f_{\text{vehicle}}^{g_{ij}}, \tag{6}$$

where ω_1 and ω_2 are coefficients, $f_{\text{totalT}}^{g_{ij}}$ represents the time required for vehicle i to merge into the mainline if it chooses the target location g_{ij}, $f_{\text{vehicle}}^{g_{ij}}$ represents the price that all vehicles need to pay in the process of merging. And

$$f_{\text{totalT}}^{g_{ij}} = t_i^{g_{ij}} - t_i^{\text{CCL}}, \tag{7}$$

where t_i^{CCL} represents the time when the vehicle i arrives at the CCL, and $t_i^{g_{ij}}$ is the ending time of the merging process of vehicle i which merges into the main road from g_{ij}. And only when the distance between the merging vehicle i and the front and rear vehicles of the potential merging position g_{ij} meets (8), the vehicle i can merge into the main road.

(a)

▼ Self-computation

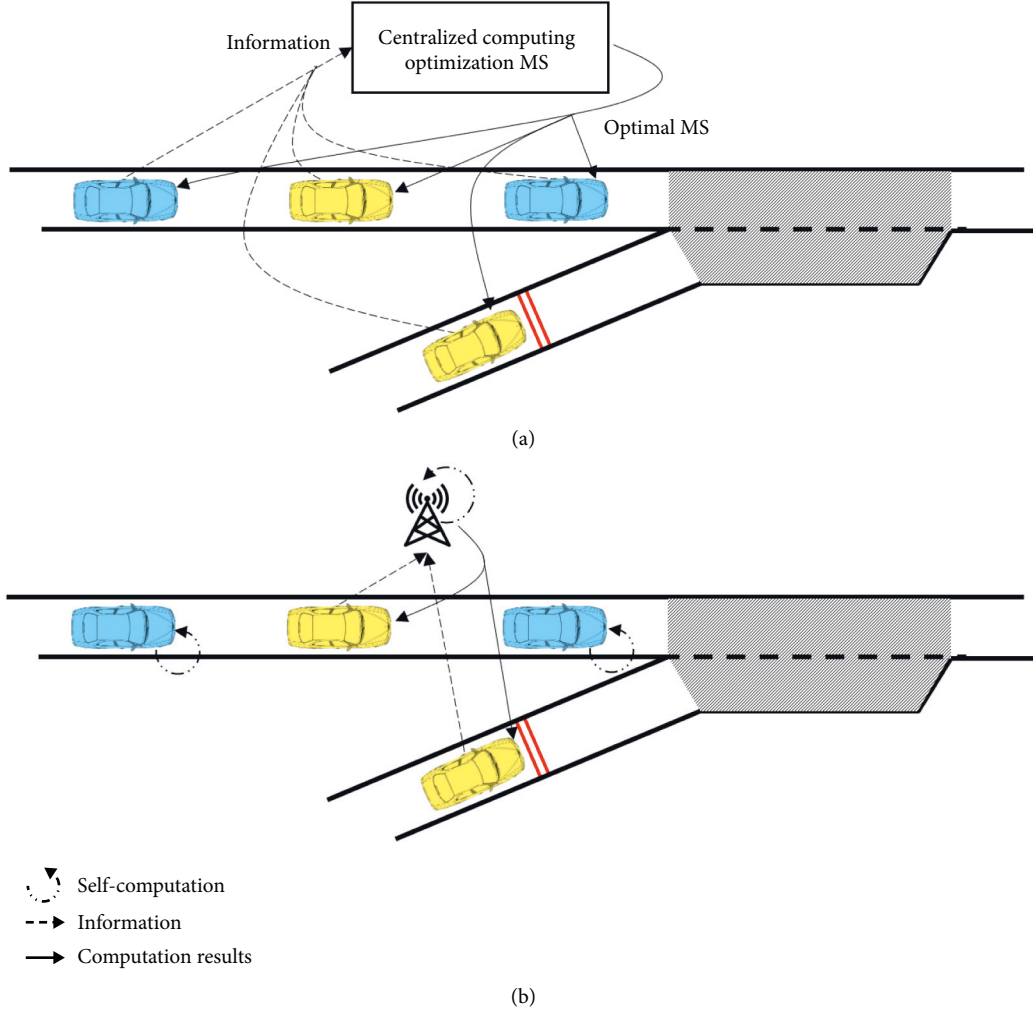- - ▶ Information

—▶ Computation results

(b)

FIGURE 4: Different calculation structures: (a) the central calculation structure of traditional merging sequence optimization; (b) the hybrid calculation structure of merging sequence optimization method based on the reverse auction.

$$\begin{cases} p_j - p_i = \Delta p_{j,i_{des}}, \\ p_i - p_{j-1} = \Delta p_{i,j-1_{des}}, \end{cases} \tag{8}$$

where the $p_{j,i_{des}}$ represents the desired distance between the main-lane vehicle j and vehicle i at the on-ramp, and $p_{i,j-1_{des}}$ is the desired distance between vehicle $j-1$ and on-ramp merging vehicle i. And then,

$$f_{vehicle}^{g_{ij}} = \sum_{k=1}^{m+i} \int_{t_i^{CCL}}^{t_i^{g_{ij}}} \left(f_k^{safe} \left(x_k(t), x_{k_{des}}(t) \right) + f_k^{fuel} \left(v_k(t), a_k(t) \right) \right) dt, \tag{9}$$

where $f_k^{safe}(x_k(t), x_{k_{des}}(t))$ and $f_k^{fuel}(v_k(t), a_k(t))$ are the safety and fuel consumption functions of the vehicle $k \in \{1, 2, \ldots, m+i\}$ in the process of merging. And

$$f_k^{safe} \left(x_k(t), x_{k_{des}}(t) \right) = \left(x_k(t) - x_{k_{des}}(t) \right)^T \Gamma \left(x_k(t) - x_{k_{des}}(t) \right), \tag{10}$$

where the Γ is the weight matrix, and $x_{k_{des}}$ is the desired states. In this work, the fuel consumption model

$f_k^{fuel}(v_k(t), a_k(t))$ we use is the classical instantaneous fuel consumption model proposed by R. Akcelik [38].

After all the sellers $\{s_1, s_2, \ldots, s_m\}$ have given their prices $\{bid_i^{g_{i1}}, bid_i^{g_{i2}}, \ldots bid_i^{g_{im}}\}$, that sellers' revenue can be expressed as

$$RE_{ij}^s = \frac{1}{bid_i^{g_{ij}}}. \tag{11}$$

On the other hand, in order to successfully complete the merging, we assume that the buyer's revenue is 0, that is $RE_{ij}^b = 0$. Therefore, the total revenue is expressed as

$$RE_{ij} = RE_{ij}^s + RE_{ij}^b, \tag{12}$$

where the $RE_{ij} \in RE_i$. Then, the winner w_i^*, the corresponding control input set $U^{w_i^*}$, and the corresponding desired state set $X^{w_i^*}$ of all vehicles can be obtained through

$$\left(w_i^*, U^{w_i^*}, X^{w_i^*} \right) = \max \left\{ RE_{i1}, RE_{i2}, \ldots RE_{ij}, \ldots RE_{im} \right\}, \tag{13}$$
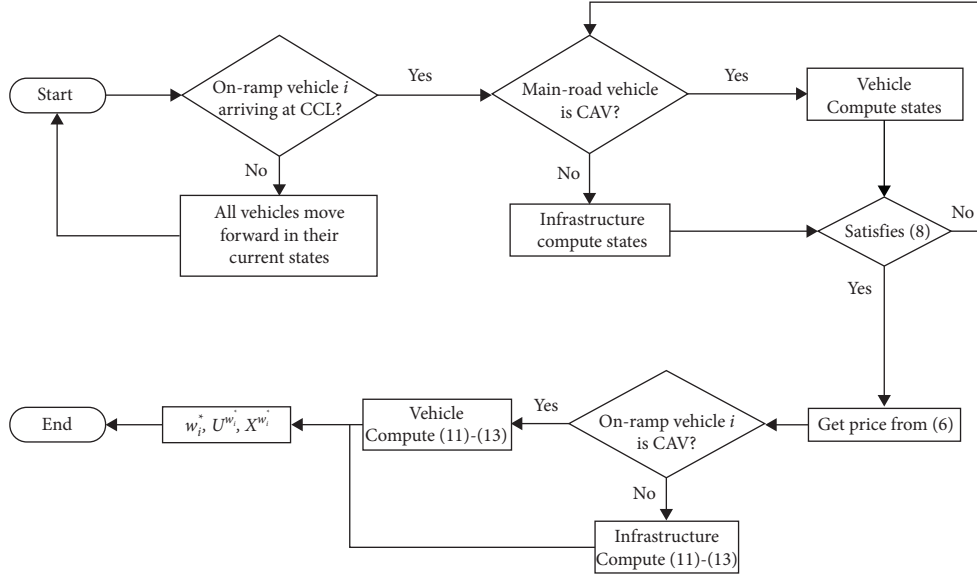
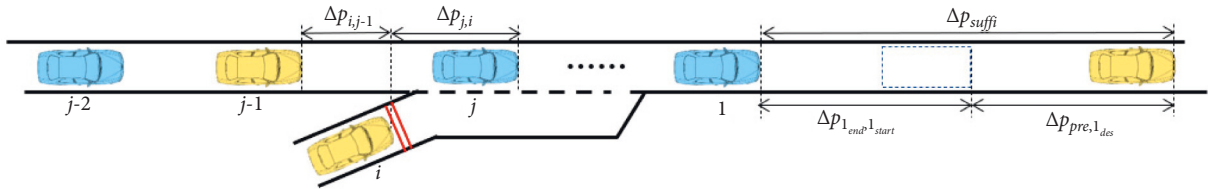FIGURE 5: Flow chart for obtaining the optimal MS.

FIGURE 6: The important assumption for realizing the merging strategy in mixed traffic and conditions for on-ramp vehicles to realize merging.

where $U^{w_i^*} = \left\{u_1^{w_i^*}, u_2^{w_i^*}, \ldots, u_m^{w_i^*}, \ldots, u_{m+n'}^{w_i^*}\right\}$ $U^{w_i^*} = \left\{u_1^{w_i^*}, u_2^{w_i^*}, \ldots, u_m^{w_i^*}, \ldots, u_{m+n'}^{w_i^*}\right\}$ and $X^{w_i^*} = \left\{x_1^{w_i^*}, x_2^{w_i^*}, \ldots, x_m^{w_i^*}, \ldots, x_{m+n'}^{w_i^*}\right\}$. After obtaining $U^{w_i^*}$, the onboard controller on the CAV can change the state of the vehicle. However, the driver in CHV can only intuitively understand information such as position and velocity. Therefore, $X^{w_i^*}$ needs to be obtained when optimizing MS. This also ensures that the method in this article can be used in mixed traffic situations. At this time, the optimal MS of the merging vehicle i is determined. For example, if $w_i^* = 2$, then the optimal MS of vehicle i is $1 \longrightarrow 2 \longrightarrow i \longrightarrow 3 \longrightarrow \ldots \longrightarrow m$. Ultimately, the process of obtaining optimal MS is shown in Figure 5. Because the MS optimization method in this article refers to the reverse auction, the biggest difference in the structure of the method is the distribution of calculations of different merging sequences to the corresponding main-lane vehicles.

3.2. Merging Strategy for Heterogeneous Vehicles.
In contrast to the previous work [30] in which all vehicles were CAVs, in this subsection, we consider the on-ramp cooperative merging when CAV and CHV are mixed. Considering the differences between CAV and CHV, we combine the virtual vehicle theory to ensure the multivehicles collaborative

completion of merging by designing virtual vehicles that heterogeneous vehicles follow during the collaborative merging process.

Figure 6 shows an important assumption for realizing the merging strategy and the conditions for the on-ramp vehicle to realize the merging. In order to ensure the smooth implementation of the merging, we set that the leading vehicle 1 of the downstream vehicles participating in the collaboration has sufficient space Δp_{suffi} for adjustment, $\Delta p_{\text{suffi}} \geq \Delta p_{1_{\text{end}},1_{\text{start}}} + \Delta p_{\text{pre},1_{\text{des}}} \geq \Delta p_{j,i_{\text{des}}} + \Delta p_{\text{pre},1_{\text{des}}}$. The dotted rectangle in the figure represents the possible position of the leading vehicle 1 at the time when the on-ramp vehicle completes the merging. $\Delta p_{1_{\text{end}},1_{\text{start}}}$ is the relative distance coordinated by vehicle 1 in the cooperative merging process. $\Delta p_{\text{pre},1_{\text{des}}}$ is the expected distance when vehicle 1 follows its preceding vehicle. $\Delta p_{j,i_{\text{des}}}$ is the desired following distance of on-ramp vehicle i following vehicle j after merging into the main road. In the figure, $\triangle p_{ji}$ is the distance between the on-ramp merging vehicle i and the downstream vehicle j at the target merging position, $\triangle p_{ji} = p_j - p_i$. And $\triangle p_{i,j-1}$ is the distance between the on-ramp merging vehicle i and the upstream vehicle $j-1$ at the target merging position, $\triangle p_{i,j-1} = p_i - p_{j-1}$. When both $\triangle p_{ji}$ and $\triangle p_{i,j-1}$ satisfy (8), the on-ramp merging vehicle i can enter the main road without collision. This also means that the on-ramp merging vehicle i has completed the merging process at this time.
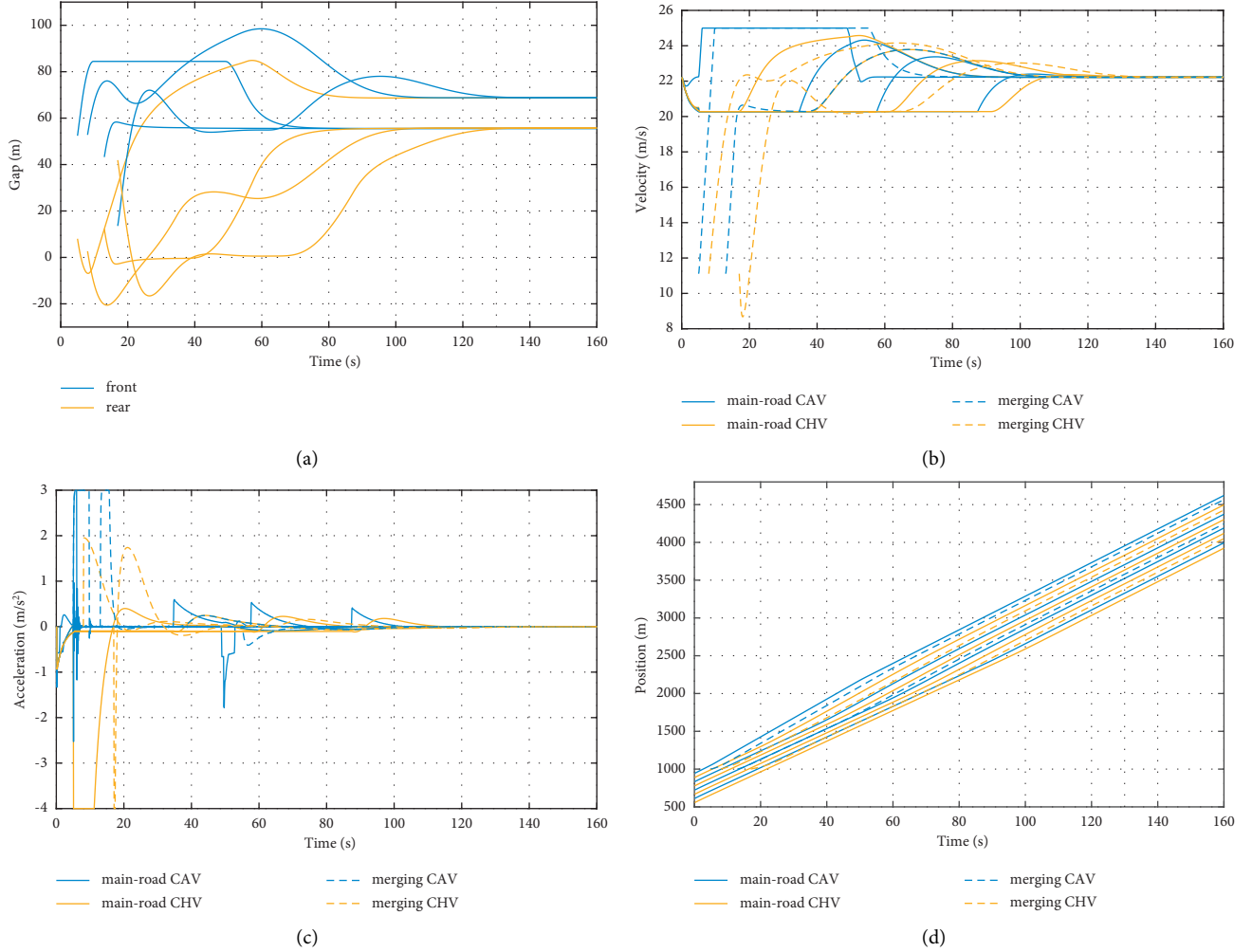
(a)

(b)

(c)

(d)

FIGURE 7: Change of vehicles' status in the proposed strategy. (a) The change of distances between on-ramp vehicles. (b) The different velocities of all vehicles. (c) The different acceleration rates of cooperative vehicles. (d) All vehicles' positions.

To better understand the proposed strategy, we have defined and explained some concepts and preconditions:

(1) The space $\triangle P_{\text{suffi}}$ before the 1st mainline downstream vehicles is sufficient as shown in Figure 6. In the strategy, the mainline downstream vehicles are required to accelerate to adjust a cooperative space for the on-ramp vehicle to merge. In order to ensure the realization of the strategy, we assume that there is sufficient and safe space $\triangle P_{\text{suffi}}$ before the 1st mainline downstream vehicle.

(2) Mainline cooperative vehicles are all subject to coordinated control. In the strategy, mainline downstream vehicles are required to perform operations such as acceleration. Unlike the forced deceleration of mainline upstream vehicles, mainline downstream vehicles are likely to be unwilling to accelerate. We assume that all vehicles are subject to the control of the proposed strategy. This ensures that the strategy of this article can be realized. In actual traffic, we can encourage mainline downstream vehicles to obey coordinated control through incentives such as economic incentives.

3.2.1. The Control of Heterogeneous Vehicles.

There are two types of vehicles, CAV and CHV, in our research. There are obvious differences between the two vehicles in terms of a car following methods. In many existing studies, CAV implements a car following under the control of a designed tracking controller. Although CHV realizes the vehicle networking function, it is still controlled by the driver.

(1) The Control of CAV. When designing the CAV controller, we considered the safety and fuel consumption of the vehicle in the process of merging. Therefore, the objective function and constraints of CAV are

$$\min J_{\text{cav}} = f_{\text{cav}}^{\text{safe}} + f_{\text{cav}}^{\text{fuel}},$$

$$\text{s.t.} \begin{cases} (17)-(18), & \text{if CAV is a downstream vehicle,} \\ (19)-(20), & \text{if CAV is an on-ramp merging vehicle,} \\ (21)-(22), & \text{if CAV is an upstream cooperative vehicle.} \end{cases}$$

$$(14)$$

Depending on the CAVs' velocity, acceleration, etc., $f_{\text{cav}}^{\text{safe}}$ and $f_{\text{cav}}^{\text{fuel}}$ can be obtained. To solve it, we use the particle
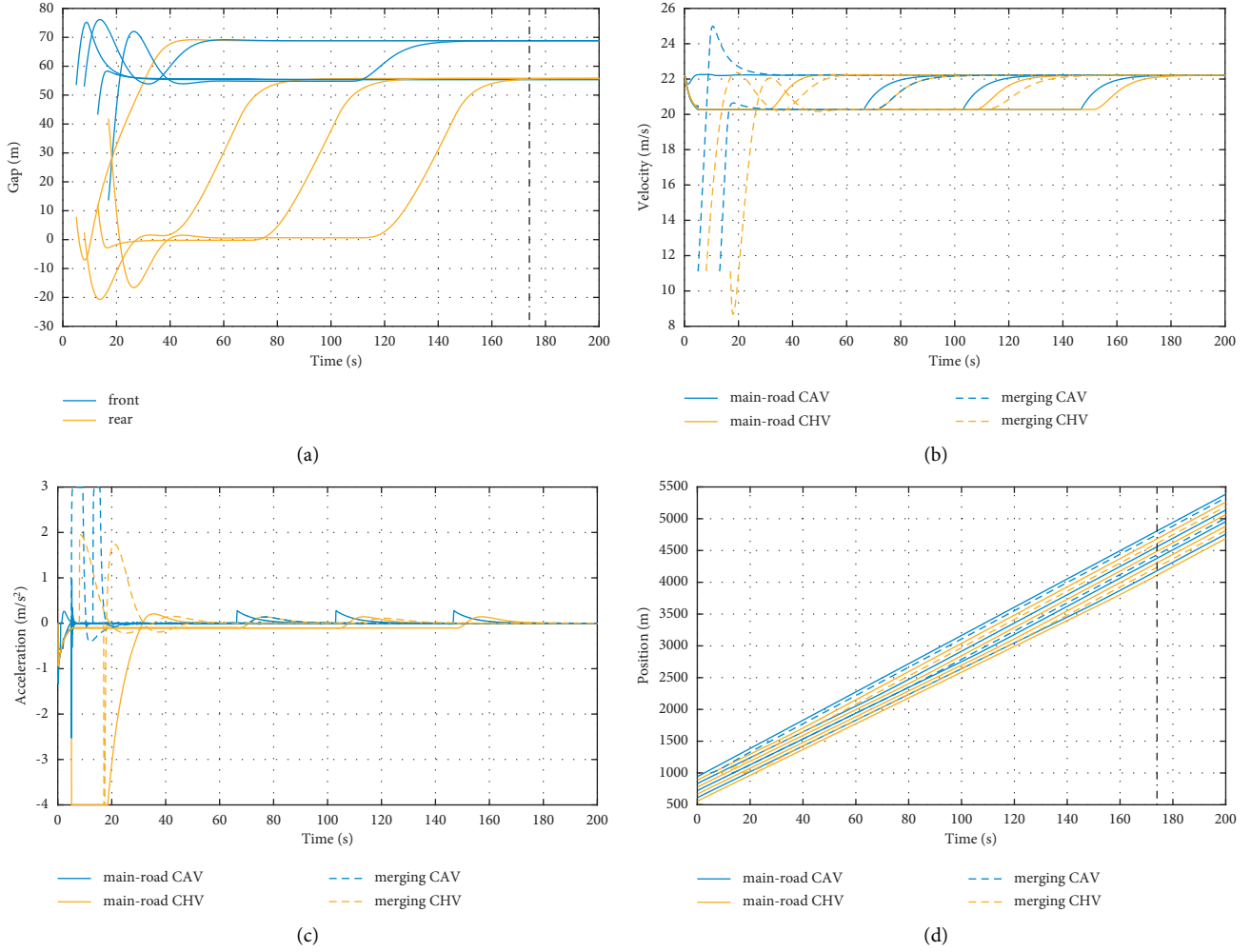
(a)

(b)

(c)

(d)

FIGURE 8: Change of vehicles' status in conventional strategy with constraints of velocities. (a) The change of distances between on-ramp vehicles. (b) The different velocities of all vehicles. (c) The different acceleration rates of all vehicles. (d) All vehicles' positions.

swarm algorithm (PSO). Moreover, the penalty function is used to deal with vehicle constraints.

(2) The Control of CHV. In the work, we choose the intelligent driver model (IDM) to characterize the car following behavior of CHV. The acceleration of the vehicle is given as

$$
\frac{\mathrm{d}v_{chv}(t)}{\mathrm{d}t}
= a_{\max}\left[1 - \left(\frac{v_{chv}(t)}{v_{\max}}\right)^4 - \left(\frac{\Delta p^*_{chv}\big(v_{chv}(t), \Delta v_{chv,vir}(t)\big)}{\Delta p_{chv,vir}(t)}\right)^2\right], \tag{15}
$$

where $\Delta p^*_{chv}(v_{chv}(t), \Delta v_{chv,vir}(t))$ is the desired gap of the driver, and $\Delta v_{chv,vir}(t)$ and $\Delta p_{chv,vir}(t)$ are the difference velocity and distance between the vehicle and its virtual vehicle. And

$$
\begin{aligned}
&\Delta p^*_{chv}\big(v_{chv}(t), \Delta v_{chv,vir}(t)\big)\\
&= p_0 + \max\left(0, Tv_{chv}(t) + \frac{v_{chv}(t)\Delta v_{chv,vir}(t)}{\sqrt{a_{\max}b}}\right),
\end{aligned} \tag{16}
$$

where b is the deceleration of the vehicle.

3.2.2. The Virtual Vehicles Corresponding to Cooperative Vehicles. In this article, the main-lane cooperative vehicles and on-ramp merging vehicles in the cooperative merging complete the merging by tracking virtual vehicles. And other vehicles move forward by following their preceding vehicles. Under this strategy, the acquisition of virtual vehicles is an important part. Because the proposed strategy requires the downstream vehicles to adjust their velocities, we need to design the virtual vehicles of these vehicles.

(1) For Downstream Vehicles. First, let us get the virtual vehicle of the downstream vehicle. According to the above description, we can get

$$
\begin{aligned}
p_{j_{vir}}(t) &= p_{j_{init}} + v_{j_{init}} \cdot t + \omega_3 \Delta p_{ji_{des}} + \Delta p_{vir,j},\\
\Delta p_{ji_{des}} &= l_{veh} + \Delta p_0 + v_{i_{des}} \cdot T,\\
\Delta p_{vir,j} &= l_{veh} + \Delta p_0 + v_{j_{init}} \cdot T,\\
v_{j_{vir}}(t) &= v_{j_{init}},\\
a_{j_{vir}}(t) &= a_{j_{init}},
\end{aligned} \tag{17}
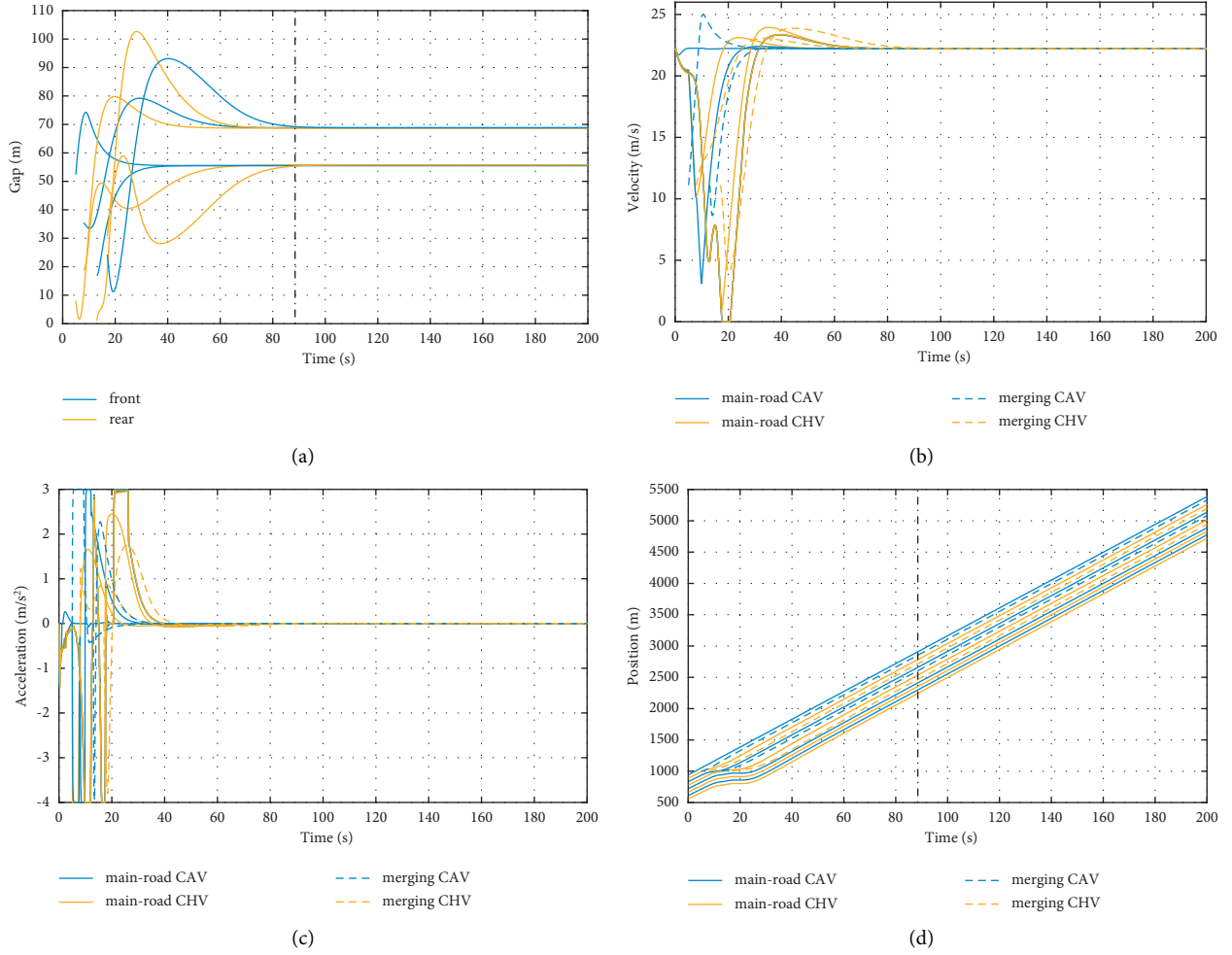$$

(a)

(b)

(c)

(d)

FIGURE 9: Change of vehicles' status in conventional strategy without velocity constraints. (a) The change of distances between on-ramp vehicles. (b) The velocities of all vehicles. (c) The acceleration rates of all vehicles. (d) All vehicles' positions.

TABLE 1: Experimental results of the cooperative merging of vehicles in different strategies.

Items	Strategy		
	Fully proactive cooperative merging	Conventional strategy with constraints	Conventional strategy without constraints
The main-road LOS	A	A	B
The total time for merging (s)	130	174	88.5
The total fuel consumption required by all vehicles during the merging process (mL)	342.63	427.79	267.49

where $p_{j_{init}}$ is the initial position of the downstream vehicle j, $v_{j_{init}}$ is the initial velocity, $\Delta p_{j_{ides}}$ is the desired distance between the on-ramp merging vehicle i and downstream vehicle j, $\omega_3 \Delta p_{ji_{des}}$ is the distance for downstream vehicles of the target merging position to achieve cooperative merging through acceleration, $\omega_3 = 0.5$ is the coefficient, $\Delta p_{vir,j}$ is the desired distance between the downstream vehicle j and its corresponding virtual vehicle, l_{veh} is vehicles' length, Δp_0 is the distance when the vehicle is static, $v_{i_{des}}$ is the desired velocity of on-ramp merging vehicle i, T is the time headway, $v_{j_{init}}$ is the initial velocity of vehicle j, and $a_{j_{init}}$ is the initial acceleration.

Considering the physical characteristics of vehicles and the impact of merging behavior, the vehicle j is subject to

$$a_{j_{min}} \leq a_{j_{vir}}(t) \leq a_{j_{max}},$$
$$v_{j_{init}} \leq v_{j_{vir}}(t) \leq v_{max}, \tag{18}$$

where a_{max} is the maximum acceleration, a_{min} is the minimum acceleration, and v_{max} is the main-road maximum velocity limit.

(2) For On-Ramp Merging Vehicle. Since vehicle i will follow the main-road vehicle j after it merges into the main road, we can get the virtual vehicle of the on-ramp vehicle i as
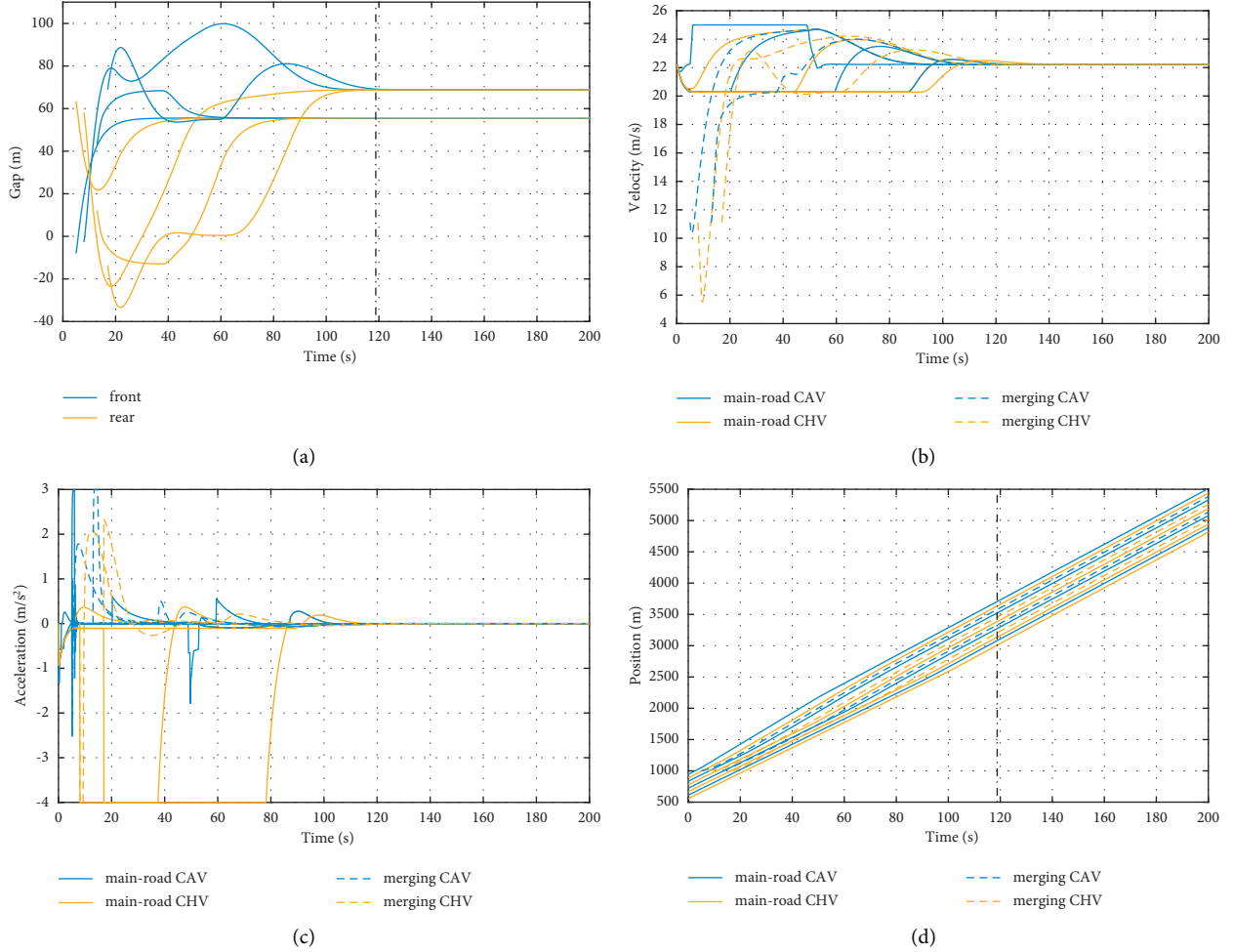
(a)

(b)

(c)

(d)

FIGURE 10: Change of vehicles' status in FPCMS with optimization of FIFO-MS. (a) The change of distances between on-ramp vehicles. (b) The velocities of all vehicles. (c) The acceleration rates of all vehicles. (d) All vehicles' positions.

$$p_{i_{vir}}(t) = p_j(t),$$
$$a_{i_{vir}}(t) = a_j(t), \tag{19}$$
$$v_{i_{vir}}(t) = v_j(t).$$

Moreover, the velocity and acceleration of the on-ramp merging vehicle are also subject to

$$v_{i_{\min}} \le v_{i_{vir}}(t) \le v_{\max},$$
$$a_{i_{\min}} \le a_{i_{vir}}(t) \le a_{i_{\max}}, \tag{20}$$

where $v_{i_{\min}}$ is the minimum speed of the on-ramp vehicle i.

(3) For Upstream Cooperative Vehicle. After determining the virtual vehicles of the downstream vehicle and the on-ramp merging vehicle, we can obtain the state virtual vehicle of the upstream cooperative vehicle as

$$p_{j-1_{vir}}(t) = p_j(t) - \Delta p_{ji_{de\,s}},$$
$$a_{j-1_{vir}}(t) = a_j(t), \tag{21}$$
$$v_{j-1_{vir}}(t) = v_j(t),$$

Similarly, the constraints of vehicle $j - 1$ are

$$a_{j-1_{\min}} \le a_{j-1_{vir}}(t) \le a_{j-1_{\max}},$$
$$v_{j-1_{\min}} \le v_{j-1_{vir}}(t) \le v_{\max}. \tag{22}$$

4. Simulation and Analysis

In this section, the effectiveness and advancement of our proposed method are verified. We use MATLAB 2019a to perform simulation experiments on a personal computer. The computer used in this paper is configured with Intel(R) Core(TM) i5-8500 CPU, 8G memory, and Win10 professional operating system.

In the work, the state of traffic is described by using the level of service (LOS) in the Highway Capacity Manual (HCM) [39]. In the classification of LOS, when the velocity range of free flow is 75 km/h to 90 km/h, as long as the average velocity is greater than 72 km/h, the service level is *A*. Therefore, we assume that the main-lane vehicles' initial velocity is 80 km/h. We set the upstream vehicles' minimum speed as 73 km/h. And the on-ramp vehicles' initial velocity is 40 km/h, vehicles' length is $l_{veh} = 6$ m, $\tau = 0.1$ s, and the
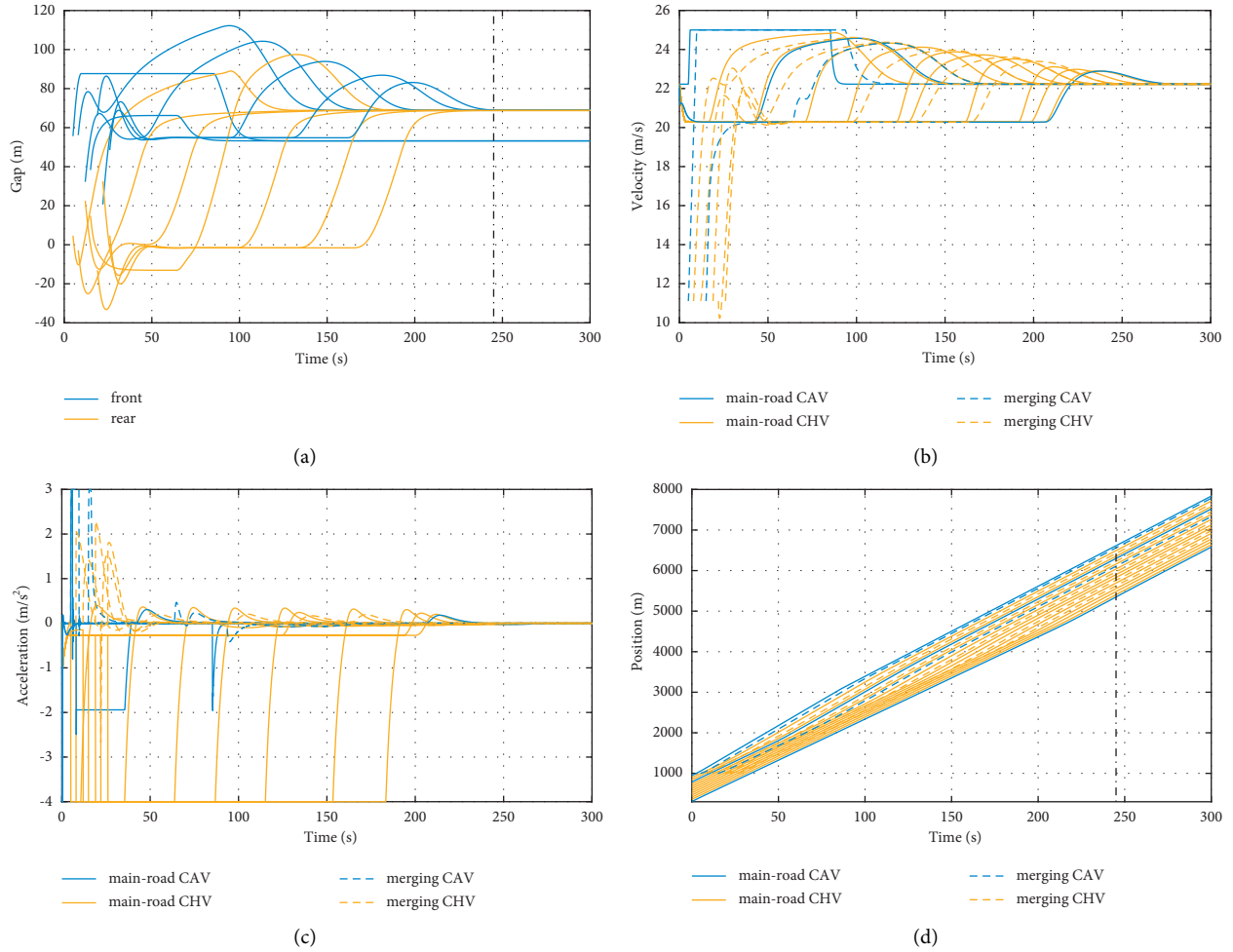
(a)

(b)

(c)

(d)

FIGURE 11: Change of vehicles' status in FPCMS for the computation time of optimization FIFO-MS. (a) The change of distances between on-ramp vehicles. (b) The different velocities of all vehicles. (c) The acceleration rates of all vehicles. (d) All vehicles' positions.

initial acceleration of all vehicles is $0 \, \text{m/s}^2$. According to the value range given in [40], the values of the parameters in IDM in this paper are as follows: the maximum acceleration is $3 \, \text{m/s}^2$, the minimum acceleration is $-4 \, \text{m/s}^2$, the static distance between the vehicle $l_0 = 5 \, \text{m}$, headway $T = 2 \, \text{s}$, the weights $\omega_1 = 2\omega_1 = 2$ and $\omega_2 = 1$, and Γ is an identity matrix.

4.1. Effectiveness and Comparison of Cooperative Merging Strategy in Mixed Traffic. In this section, we verify the feasibility of the proposed strategy in mixed traffic to ensure cooperative merging through a simulation experiment firstly. Then, the experimental results of this strategy are compared with the simulation results of the conventional strategy under the same experimental settings. There are eight main-road vehicles and four on-ramp vehicles. These on-ramp vehicles start their merging behavior at 5th, 8th, 13th, and 17th seconds, respectively. The experimental results of using the proposed strategy and the conventional strategy in mixed traffic are shown in Figures 7–9, respectively.

Figure 7(a) shows the distance between the merging vehicle and the downstream vehicle of the target merging position and the distance between the merging vehicle and

the upstream vehicle of the target merging position. From the figure, we find that the front distance and rear distance of the merging vehicle reach the desired distance at the 130th second. This means that the merging vehicle merges into the main road at this time. Figure 7(b) shows the velocity changes of all vehicles during the merging process. We can find that the velocity changes of the vehicles in the merging process strictly comply with the velocity constraints we designed. This ensures that the merging process will not worsen the traffic on the main road. Through statistics, the vehicles' average velocity is $21.82 \, \text{m/s} \approx 78.55 \, \text{km/h}$. This shows that during the merging process, the main-lane LOS remains at level *A*. From Figure 7(c), we can find that the acceleration of all vehicles is within the constraint range. Under the strategy of this article, all vehicles are successfully merged finally.

In the conventional strategy, the downstream vehicles' velocities always remain unchanged, and only the velocity of the upstream vehicles changes. These conventional cooperative merging strategies fall into two main categories: main-road upstream vehicles considering velocity constraints and main-road upstream vehicles that have no speed constraints.
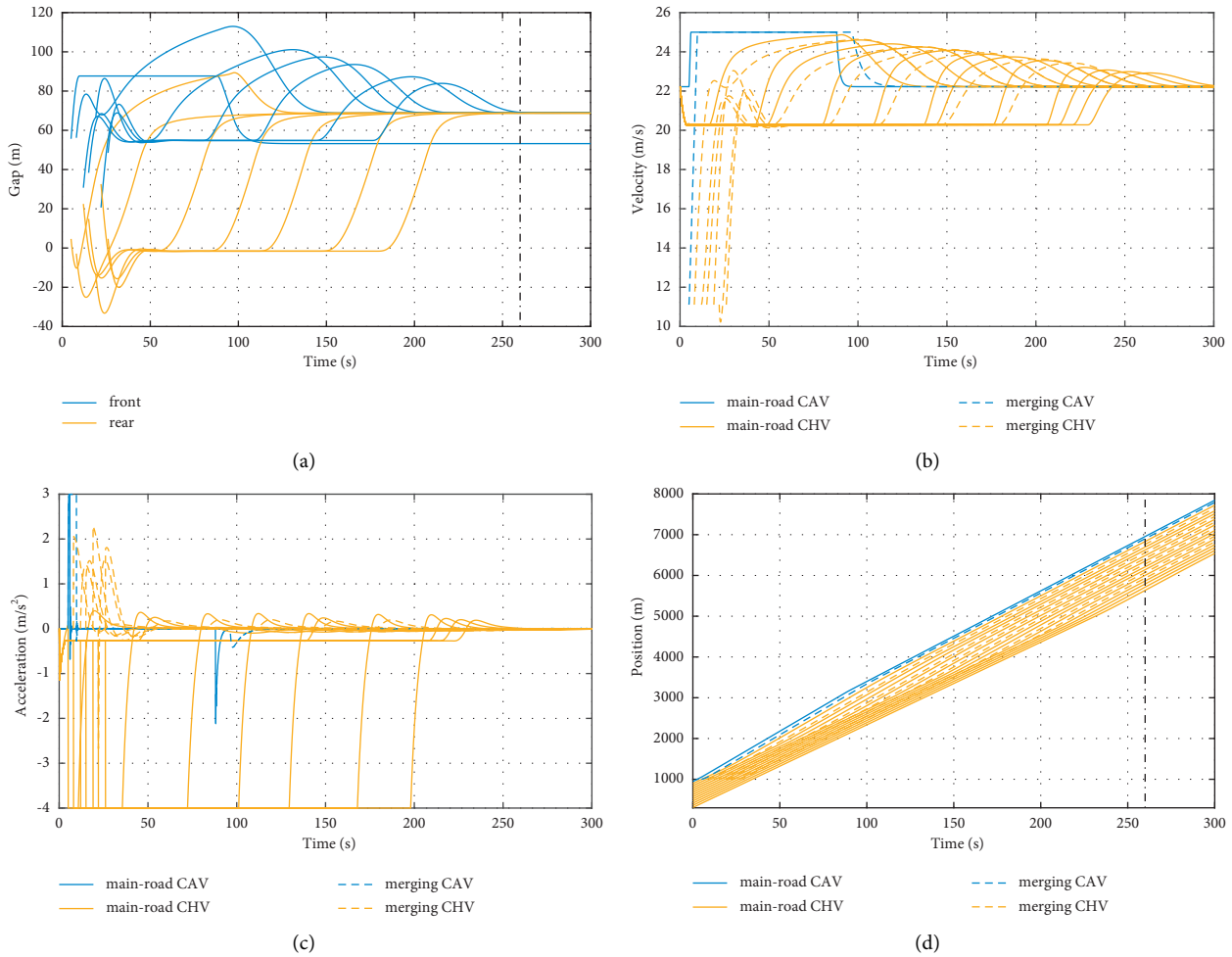
(a)

(b)

(c)

(d)

FIGURE 12: Penetration of CAV is 0.1. (a) The change of distances between on-ramp vehicles. (b) The velocities of all vehicles. (c) The acceleration of vehicles. (d) All vehicles' positions.

Figure 8 shows the experimental results of considering the velocity constraints for main-road upstream cooperative merging vehicles. It can be known from Figure 8(a) that, with the cooperation of upstream vehicles, the distance between vehicles will eventually meet the conditions of merging. Figure 8(b) shows the velocity changes of all vehicles in the process of merging. From the figure, we can see that the downstream vehicles' velocities remain unchanged from beginning to end. In the process of merging, the acceleration of all vehicles still obeys the constraints, and the result is shown in Figure 8(c). In the end, under the conventional strategy, all merging processes ended at 174th second. All merging vehicles successfully merged into the main road as shown in Figure 8(d).

Figure 9 shows the experimental results of the cooperative merging of main-road upstream vehicles without speed constraints. It can be seen from Figure 9(a) that the vehicles on the main road can successfully adjust the distance between vehicles that satisfy the merging of on-ramp vehicles when the velocity constraints are not considered for main-road upstream vehicles. However, the upstream traffic status of the main road is very much affected by the merging behavior during the merging process of on-ramp vehicles. As shown in Figures 9(b) and 9(c), during the merging process of on-ramp vehicles,

main-road upstream vehicles even appear to stop, and the acceleration of all vehicles is within the constraint range. Finally, all the on-ramp vehicles are successfully merged into the main road, as shown in Figure 9(d).

The data statistics of all experiments are shown in Table 1.

Considering the constraints, in the conventional on-ramp merging strategy, the average velocity of vehicles is 21.21 m/s ≈ 76.36 km/h, and the corresponding LOS level is A. Although the LOS in the two strategies is A level, the average vehicle velocity in this proposed strategy is significantly higher. When the conventional cooperative merging strategy does not consider the velocity constraints of main-road upstream vehicles, the average velocity of the main-road vehicles is 19.78 m/s ≈ 71.21 km/h, and the corresponding LOS level is B. Compared with the proposed strategy, when the velocity constraints of main-road upstream vehicles are not considered, the conventional cooperative merging strategy has a very serious adverse impact on the main-road traffic from the merging behavior. Comparing the time required for multivehicle merging under these strategies, we can find that the merging efficiency of the strategy proposed in this paper has increased by
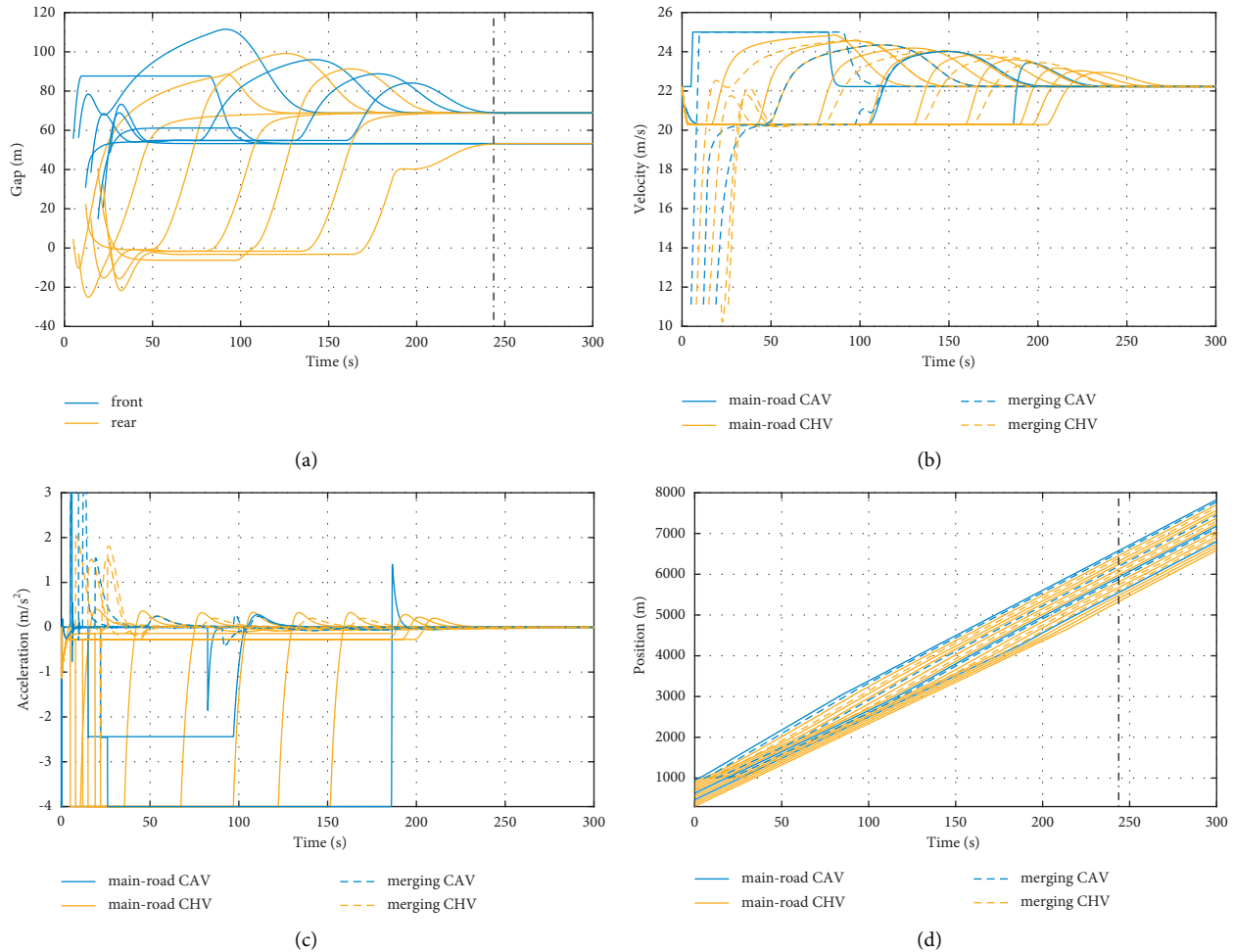
(a)

(b)

(c)

(d)

Figure 13: Penetration of CAV is 0.3. (a) The change of distances between on-ramp vehicles. (b) The velocities of all vehicles. (c) The acceleration rates of vehicles. (d) All vehicles' positions.

25.29%. Then, we compared the total fuel consumption of all vehicles in the merging process under different strategies. We find that the proposed strategy in this paper reduces the total fuel consumption by 19.91% compared to the conventional cooperative merging strategy considering the velocity constraints. By comparison, we found that although the acceleration of the vehicles in the proposed strategy fluctuates more frequently, the cooperation of the proposed strategy takes less time than the conventional strategy considering the constraints of velocity, which makes the fuel consumption of the proposed strategy in the whole cooperative merging process less than the conventional strategy considering the constraints of velocity. Although the conventional cooperative merging strategy does not consider the velocity constraints of main-road upstream vehicles that can make the on-ramp vehicles take less time to complete the merging process and the fuel consumption is reduced, it can amplify the bad impact of the merging behavior on the main-road traffic. When the conventional cooperative merging strategy does not consider the velocity constraints of main-road upstream vehicles, the main-road upstream vehicles will be affected by merging of on-ramp vehicles, and the LOS level of the main

road will be reduced to B. In serious cases, traffic congestion may even occur on the upstream main road.

Finally, in terms of the span of the merging area, these strategies all require the merging area spans more than one kilometer, as shown in Figures 7(d), 8(d), and 9(d). Although the length of the ramp can also be utilized in the cooperative merging process [25], the long span of the merging zone is likely to make it difficult to determine the merging point and increase the uncertainty of the cooperative merging behavior of vehicles. Therefore, it is necessary to optimize the span of the merging area required in future research work. However, the proposed strategy is significantly effective in mitigating the impact of merging behavior on main-road traffic.

4.2. The Effectiveness of Optimal FIFO-MS Method. In this section, we verify the effectiveness of the MS optimization method proposed in this paper. After adopting the merging sequence optimization method proposed in this paper, the experimental results of multivehicle merging are shown in Figure 10. It can be seen from Figure 10(d) that the optimized sequence of multivehicle merging in this simulation
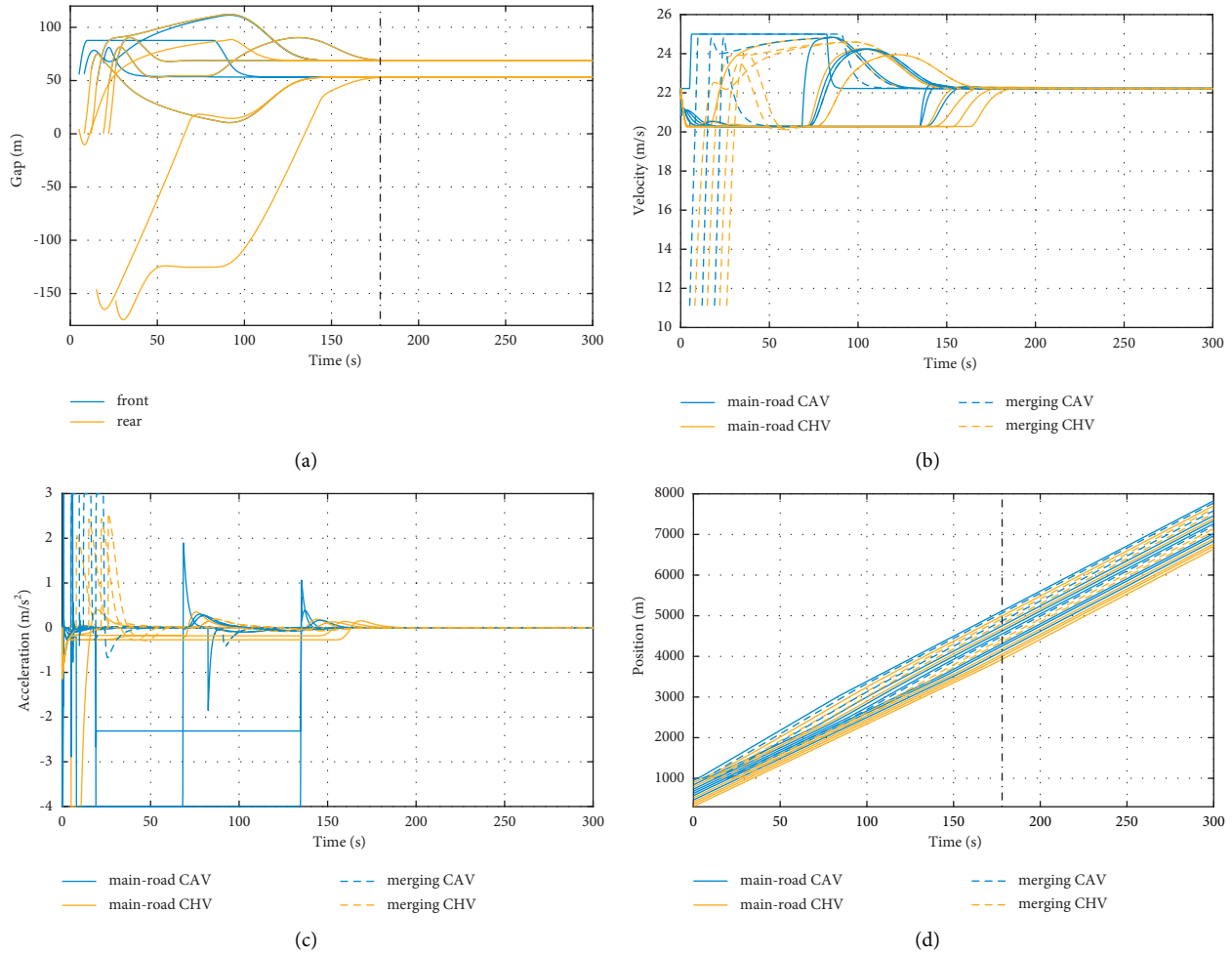
(a)

(b)

(c)

(d)

FIGURE 14: Penetration of CAV is 0.5. (a) The change of distances between on-ramp vehicles. (b) The velocities of all vehicles. (c) The acceleration rates of vehicles. (d) All vehicles' positions.

experiment is $1 \longrightarrow 2 \longrightarrow 1' \longrightarrow 3 \longrightarrow 2' \longrightarrow 4 \longrightarrow 3' \longrightarrow 5 \longrightarrow 4' \longrightarrow 6 \longrightarrow 7 \longrightarrow 8$. From Figure 7(d), we can know that the original merging sequence is $1 \longrightarrow 1' \longrightarrow 2 \longrightarrow 2' \longrightarrow 3 \longrightarrow 4 \longrightarrow 3' \longrightarrow 5 \longrightarrow 6 \longrightarrow 4' \longrightarrow 7 \longrightarrow 8$. The optimized merging sequence is different from the original merging sequence.

After optimizing the merging sequence, the vehicles' average velocity during the process is 21.85 m/s ≈ 78.66 km/h. This average velocity still corresponds to the A-level LOS. It shows that the merging sequence obtained by the merging sequence optimization method in this paper can still ensure that the merging process will not cause traffic congestion on the main road. At the same time, after optimizing the merging sequence, it can be known from Table 2 that the entire merging process is completed at 118.8[th] seconds. Compared with the original merging sequence, the optimized merging sequence saves 8.62% of time. In terms of fuel consumption of all vehicles during the merging process, the optimized merging sequence saves 11.67% compared to the original merging sequence.

4.3. Comparison between the Novel and the Conventional MS Optimization Method

4.3.1. Computation Time Required to Calculate the Optimal Sequence.
In this section, we first count the time required to obtain the best merging sequence based on the negotiation and reward in the method of this paper. Then, we compare this time with the time it takes to obtain the optimal merging sequence based on the conventional merging sequence optimization framework.

In this experiment, the number of main-lane vehicles is 13, and the number of on-ramp vehicles is 7. These on-ramp vehicles start their merging behavior at 5th, 8th, 12th, 15th, 19th, 22th, and 26th seconds, respectively. The experimental results of multivehicle merging are shown in Figure 11. From the results, we can find that the optimal FIFO-MS is $1 \longrightarrow 1' \longrightarrow 2 \longrightarrow 2' \longrightarrow 3 \longrightarrow 4 \longrightarrow 3' \longrightarrow 5 \longrightarrow 4' \longrightarrow 6 \longrightarrow 5' \longrightarrow 7 \longrightarrow 8 \longrightarrow 6' \longrightarrow 9 \longrightarrow 7' \longrightarrow 10 \longrightarrow 11$.

By counting the computation time required for the optimal merging sequence, we obtain the following: the average computation time required to negotiate and reward
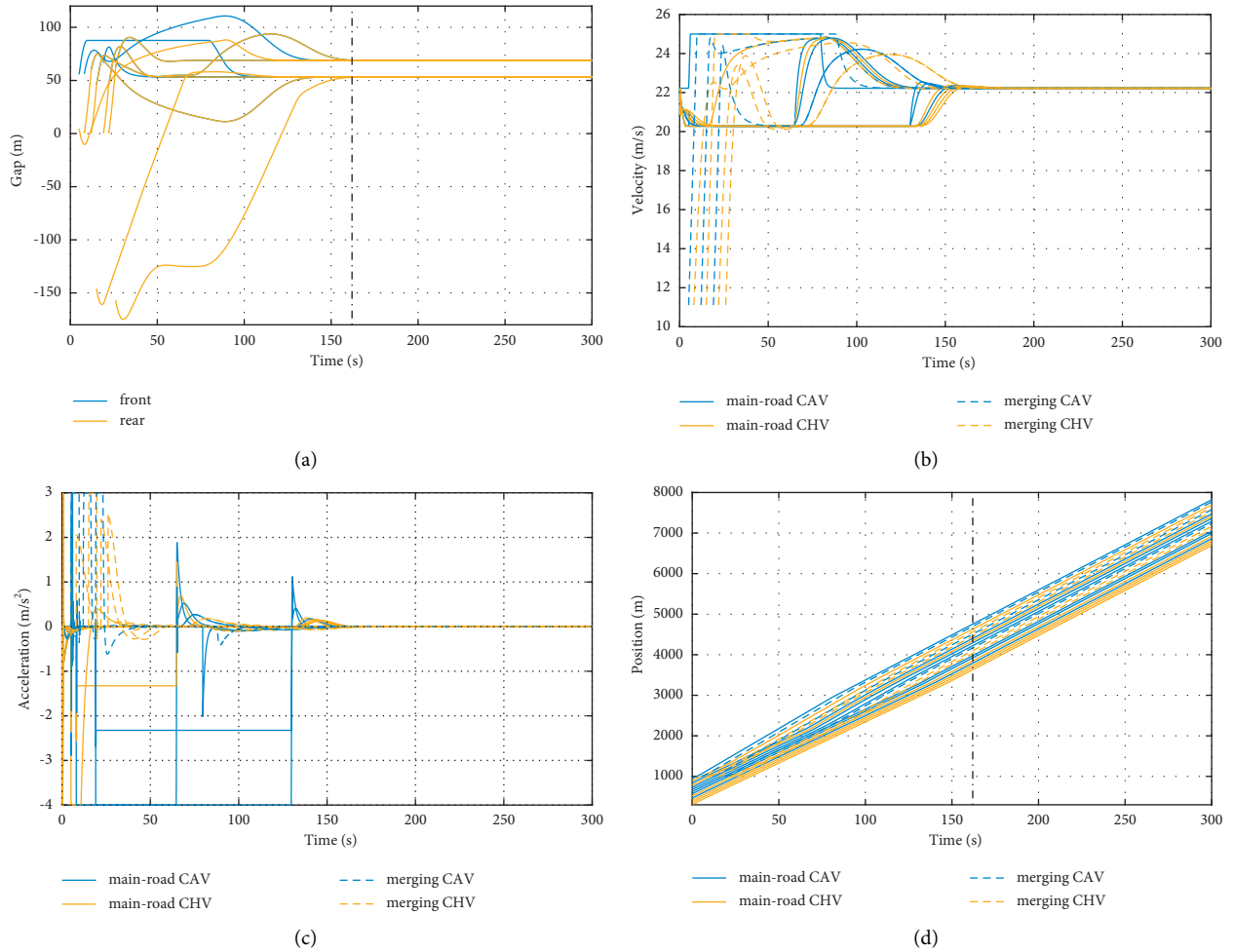
(a)

(b)

(c)

(d)

FIGURE 15: Penetration of CAV is 0.7. (a) The change of distances between on-ramp vehicles. (b) The velocities of all vehicles. (c) The acceleration rates of vehicles. (d) All vehicles' positions.

the merging sequence method proposed in this paper is 34.71 ms, and the average computation time of the conventional centralized optimization framework is 39.62 ms.

Through comparison, in this simulation experiment, the average computation time of the merging sequence optimization method in this paper is 0.06 s less than the computation time required for the conventional centralized optimization merging sequence, and the efficiency is increased by 12.39%.

It can be seen that the proposed method based on negotiation and reward in the reverse auction can obtain the optimal MS more quickly to ensure the realization of the cooperative merging of mixed traffic.

4.3.2. Influence of CAV Penetration on Computation Time. In this section, we conduct several experiments with different CAV penetration rates in mixed traffic. With the data from these experiments, we mainly analyze the effect of different CAV permeability in mixed traffic on the time required for the negotiation and reward process in the method of this paper.

In this experiment of the subsection, the number of vehicles participating in the cooperative merging and the start-merging time of the on-ramp vehicles is the same as those in Section 4.3.1. The only difference is that the proportion of CAV in the experiment in this section is changing. In order to explore the influence of CAVs' penetration in mixed traffic on the computation of optimal FIFO-MS, we simulated experiments with the occupancy rates of CAV of 0.1, 0.3, 0.5, 0.7, and 0.9, respectively. The results of the simulation experiments are shown in Figures 12–16.

First of all, the results of Figures 12(a), 13(a), 14(a), 15(a), and 16(a) show that the optimization FIFO-MS method and the proposed strategy can still obtain the optimal FIFO-MS and realize the on-ramp vehicles' merging when the CAV penetration changes. At the same time, by comparing Figures 12(d), 13(d), 14(d), 15(d), and 16(d), we can find that the optimal MS for vehicle cooperation is different under different penetrations of CAV. This demonstrates that the penetration of CAV has some influence on the process of cooperative merging. Then, we make statistics on the data of each experiment as shown in Table 3 and compare them.
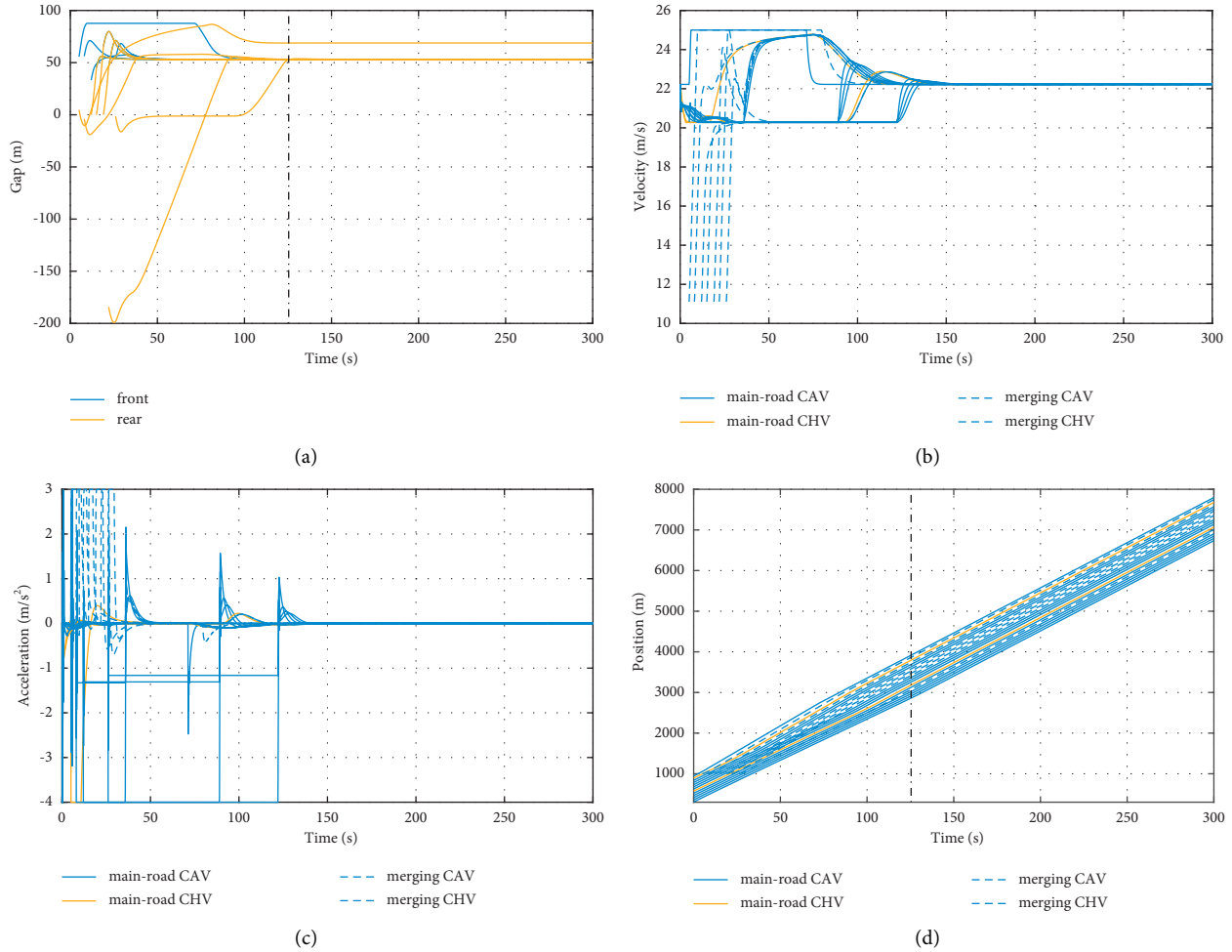
(a)

(b)

(c)

(d)

FIGURE 16: Penetration of CAV is 0.9. (a) The change of distances between on-ramp vehicles. (b) The different velocities of vehicles. (c) The different acceleration rates of vehicles. (d) All vehicles' positions.

TABLE 2: Comparison between optimal FIFO-MS and original FIFO-MS.

Items	Merging sequence	
	Optimal FIFO	FIFO
The main-road LOS	A	A
The total time for the merging process (s)	118.8	130
The total fuel consumption required by all vehicles during the merging process (mL)	302.66	342.63

When the penetration of CAV is 0.1, the merging sequence optimization method based on the reverse auction proposed in this paper needs 28.44 ms to obtain the optimal merging sequence. The conventional centralized optimization method requires 30.61 ms. In this case, the merging sequence optimization method proposed in this paper improves the efficiency of obtaining the optimal MS by 7.09%. When the penetration of CAV is 0.3, the merging sequence optimization method in this paper takes 89.68 ms, and the conventional method takes 113.47 ms. At this time, the efficiency of the method in this paper to obtain the optimal MS increased by 20.97%. When the penetration of CAV is 0.5, 0.7, and, 0.9, the negotiation and reward time required to obtain the optimal MS by the merging sequence

optimization method in this paper is 95.26 ms, 122.22 ms, and 226.2 ms, respectively. The conventional centralized optimization MS method requires 177.39 ms, 235.32 ms, and 506.58 ms, respectively. In these three cases, the method proposed in this paper reduces the time to obtain the optimal MS by 46.3%, 48.06%, and 55.35%.

Through comparison, it can be found that as the penetration of CAV increases, the average computation time to obtain the optimal MS gradually increases. This is because the CAV in this article adopts PSO optimization control in the process of merging. As the number of CAVs in the process of merging increases, it will take longer for vehicles participating in the optimization of MS to obtain the optimal MS. However, we can find that under the condition of higher

TABLE 3: Comparison of results of different optimization methods.

Penetration of CAV	Optimal FIFO-MS system framework	Average computation time (ms)	Computation efficiency	Total time for merging process (s)
0.1	Reverse auction-based optimization system	28.44	7.09%	268.5
	Centralized optimization system	30.61		
0.3	Reverse auction-based optimization system	89.68	20.97%	243.7
	Centralized optimization system	113.47		
0.5	Reverse auction-based optimization system	95.26	46.3%	178
	Centralized optimization system	177.39		
0.7	Reverse auction-based optimization system	122.22	48.06%	162
	Centralized optimization system	235.32		
0.9	Reverse auction-based optimization system	226.2	55.35%	137.3
	Centralized optimization system	506.58		

penetration of CAV, the merging sequence optimization method proposed in this paper can save more time required for computation.

Finally, through experiments, we found that when the penetration of CAV is 0.1, 0.3, 0.5, 0.7, and 0.9, the total time required for the entire cooperative merging process is 268.5 s, 243.7 s, 178 s, 162 s, and 137.3 s. This shows that the penetration of CAV has a great influence on the duration of the cooperative merging process. With the increase of penetration of CAV, the total time for on-ramp vehicles to merge into the main road gradually decreases.

5. Conclusions

This paper focuses on the optimal MS and on-ramp merging strategy of mixed traffic. Considering the importance of computation time to obtain the optimal MS, the method of optimizing the optimal MS is designed based on the reverse auction. To improve the efficiency of cooperative merging and reduce fuel consumption, an on-ramp merging strategy in mixed traffic is proposed based on the velocity change of vehicles. In addition, velocity constraints for vehicles are also taken into account in this strategy to avoid the negative effects of the merging behavior on main-lane traffic. Furthermore, the influence of CAVs' penetration in mixed traffic on the computation time of the merging sequence optimization method is analyzed. The results of numerical experiments demonstrate the effectiveness of the proposed optimization MS method to improve the optimization computation efficiency and the cooperative merging strategy to improve the merging efficiency and reduce fuel consumption.

This study emphasizes the design of the merging sequence optimization method and the proposal of a cooperative merging strategy to obtain the optimal MS faster and achieves more efficient and energy-saving merging. Also, the findings provide insights on the influence of penetration of CAV on the increase in computational efficiency of

optimizing MS where the CAVs' penetration can increase the computation efficiency. In future work, the constraint of the merging area span will be considered. And then we design the corresponding cooperative merging control strategy and merging sequence optimization method to achieve fast and energy-saving merging of on-ramp vehicles.

Data Availability

The data used to support the findings of this study are available from the corresponding author upon request.

Conflicts of Interest

The authors declare that there are no conflicts of interest regarding the publication of this paper.

Acknowledgments

References

[1] T. J. Cova and J. P. Johnson, "A network flow model for lane-based evacuation routing," *Transportation Research Part A: Policy and Practice*, vol. 37, no. 7, pp. 579–604, 2003, in English.

[2] A. I. Delis, I. K. Nikolos, and M. Papageorgiou, "Simulation of the penetration rate effects of ACC and CACC on macroscopic traffic dynamics," in *Proceedings of the IEEE 19th International Conference on Intelligent Transportation Systems (ITSC)*, pp. 336–341, Rio de Janeiro, Brazil, November 2016.

[3] R. Tu, L. Alfaseeh, S. Djavadian, B. Farooq, and M. Hatzopoulou, "Quantifying the impacts of dynamic control in connected and automated vehicles on greenhouse

gas emissions and urban NO2 concentrations," *Transportation Research Part D: Transport and Environment*, vol. 73, pp. 142–151, 2019.

[4] J. Rios-Torres and A. A. Malikopoulos, "A survey on the coordination of connected and automated vehicles at intersections and merging at highway on-ramps," *IEEE Transactions on Intelligent Transportation Systems*, vol. 18, no. 5, pp. 1066–1077, 2017.

[5] M.-R. Sonbolestan and S. Monajjem, "Optimal control of connected and automated vehicles at highway on-ramps to reduce vehicles fuel consumption and increase passenger comfort," *Control Engineering Practice*, vol. 109, Article ID 104747, 2021.

[6] M. Kyriakidis, R. Happee, and J. C. F. D. Winter, "Public opinion on automated driving: results of an international questionnaire among 5000 respondents," *Transportation Research Part F: Traffic Psychology and Behaviour*, vol. 32, pp. 127–140, 2015.

[7] R. Garreth and M. David, "Connected and automated vehicle activities in Canada," *TR news*, no. 317, pp. 10–18, 2018.

[8] H. Wei, X. Liu, L. Mashayekhy, and K. Decker, "Mixed-Autonomy Traffic Control with Proximal Policy Optimization," in *Proceedings of the IEEE Vehicular Networking Conference (VNC)*, pp. 1–8, Los Angeles, CA, USA, December 2019.

[9] D. J. Fagnant and K. Kockelman, "Preparing a nation for autonomous vehicles: opportunities, barriers and policy recommendations," *Transportation Research Part A: Policy and Practice*, vol. 77, pp. 167–181, 2015.

[10] A. Voinescu, P. L. Morgan, C. Alford, and P. Caleb-Solly, "The utility of psychological measures in evaluating perceived usability of automated vehicle interfaces – a study with older adults," *Transportation Research Part F: Traffic Psychology and Behaviour*, vol. 72, pp. 244–263, 2020.

[11] M. Alsabaan, K. Naik, and T. Khalifa, "Optimization of fuel cost and emissions using V2V communications," *IEEE Transactions on Intelligent Transportation Systems*, vol. 14, no. 3, pp. 1449–1461, 2013.

[12] W. Cao, M. Mukai, T. Kawabe, H. Nishira, and N. Fujiki, "Cooperative vehicle path generation during merging using model predictive control with real-time optimization," *Control Engineering Practice*, vol. 34, pp. 98–105, 2015.

[13] S. Jing, F. Hui, X. Zhao, J. Rios-Torres, and A. J. Khattak, "Cooperative game approach to optimal merging sequence and on-ramp merging control of connected and automated vehicles," *IEEE Transactions on Intelligent Transportation Systems*, vol. 20, no. 11, pp. 4234–4244, Article ID 8765399, 2019, in English.

[14] G. Raravi, V. Shingde, K. Ramamritham, and J. Bharadia, "Merge algorithms for intelligent vehicles," in *Next Generation Design and Verification Methodologies for Distributed Embedded Control Systems*, pp. 51–65, Springer Netherlands, Dordrecht, Netherlands, 2007.

[15] L. Li and F. Y. Wang, "Cooperative driving at blind crossings using intervehicle communication," *IEEE Transactions on Vehicular Technology*, vol. 55, no. 6, pp. 1712–1724, 2006.

[16] T. Awal, L. Kulik, and K. Ramamohanrao, "Optimal traffic merging strategy for communication- and sensor-enabled vehicles," in *Proceedings of the 16th International IEEE Conference on Intelligent Transportation Systems*, pp. 1468–1474, ITSC, The Hague, Netherlands, October 2013.

[17] J. Ding, L. Li, H. Peng, and Y. Zhang, "A rule-based cooperative merging strategy for connected and automated vehicles," *IEEE Transactions on Intelligent Transportation Systems*, vol. 21, no. 8, pp. 3436–3446, 2020.

[18] J. Wang, F. Ma, Y. Yu et al., "Optimization design of the decentralized multi-vehicle cooperative controller for freeway ramp entrance," *International Journal of Automotive Technology*, vol. 22, no. 3, pp. 799–810, 2021.

[19] M. Karimi, C. Roncoli, C. Alecsandru, and M. Papageorgiou, "Cooperative merging control via trajectory optimization in mixed vehicular traffic," *Transportation Research Part C: Emerging Technologies*, vol. 116, Article ID 102663, 2020.

[20] J. Ding, H. Peng, Y. Zhang, and L. Li, "Penetration effect of connected and automated vehicles on cooperative on-ramp merging," *IET Intelligent Transport Systems*, vol. 14, no. 1, pp. 56–64, 2020.

[21] J. Larsson, M. F. Keskin, B. Peng, B. Kulcsár, and H. Wymeersch, "Pro-social control of connected automated vehicles in mixed-autonomy multi-lane highway traffic," *Communications in Transportation Research*, vol. 1, Article ID 100019, 2021.

[22] Y. Ali, Z. Zheng, and M. M. Haque, "Modelling lane-changing execution behaviour in a connected environment: a grouped random parameters with heterogeneity-in-means approach," *Communications in Transportation Research*, vol. 1, Article ID 100009, 2021.

[23] J. Rios-Torres and A. A. Malikopoulos, "Automated and cooperative vehicle merging at highway on-ramps," *IEEE Transactions on Intelligent Transportation Systems*, vol. 18, no. 4, pp. 780–789, Article ID 7534837, 2017.

[24] Y. Zhou, M. E. Cholette, A. Bhaskar, and E. Chung, "Optimal vehicle trajectory planning with control constraints and recursive implementation for automated on-ramp merging," *IEEE Transactions on Intelligent Transportation Systems*, vol. 20, no. 9, pp. 1–12, 2018.

[25] Y. Zhou, E. Chung, A. Bhaskar, and M. E. Cholette, "A state-constrained optimal control based trajectory planning strategy for cooperative freeway mainline facilitating and on-ramp merging maneuvers under congested traffic," *Transportation Research Part C-Emerging Technologies*, vol. 109, pp. 321–342, 2019, in English.

[26] S. Karbalaieali, O. A. Osman, and S. Ishak, "A dynamic adaptive algorithm for merging into platoons in connected automated environments," *IEEE Transactions on Intelligent Transportation Systems*, vol. 21, no. 10, pp. 4111–4122, 2020.

[27] H. Li, J. Zhang, Z. Zhang, and Z. Huang, "Active lane management for intelligent connected vehicles in weaving areas of urban expressway," *Journal of Intelligent and Connected Vehicles*, vol. 4, no. 2, pp. 52–67, 2021.

[28] G. Chai, J. Cao, and S. Xu, "An optimized on-ramp metering method for urban expressway based on reinforcement learning," *Journal of Intelligent and Fuzzy Systems*, vol. 38, no. 3, pp. 2703–2715, 2020.

[29] S. Jing, X. Zhao, F. Hui, A. J. Khattak, and L. Yang, "Cooperative CAVs Optimal Trajectory Planning for Collision Avoidance and Merging in the Weaving Section," *Transportation Business: Transport Dynamics*, vol. 9, no. 1, pp. 1–18, 2020.

[30] S. Wang, M. Zhao, D. Sun, T. Zhou, and Z. Liu, "A fully cooperative merging strategy considering the impact of on-ramp merging behavior on upstream traffic," in *Proceedings of the COTA International Conference of Transportation Professionals CICTP 2021*, pp. 2578–2588, Xian, China, December 2021.

[31] W. Guo, Y. Zhang, and L. Li, "The integration of CPS, CPSS, and ITS: a focus on data," *Tsinghua Science and Technology*, vol. 20, no. 4, pp. 327–335, 2015.

[32] H. Pei, S. Feng, Y. Zhang, and D. Yao, "A cooperative driving strategy for merging at on-ramps based on dynamic programming," *IEEE Transactions on Vehicular Technology*, vol. 68, no. 12, pp. 11646–11656, 2019.

[33] W. Vickrey, "Counterspeculation, auctions, and competitive sealed tenders," *The Journal of Finance*, vol. 16, no. 1, pp. 8–37, 1961.

[34] D. M. Kreps, P. Milgrom, J. Roberts, and R. Wilson, "Rational cooperation in the finitely repeated prisoners' dilemma," *Journal of Economic Theory*, vol. 27, no. 2, pp. 245–252, 1982.

[35] https://www.nobelprize.org/prizes/economic-sciences/.

[36] P. Klemperer, "Auction theory: a guide to the literature," *Journal of Economic Surveys*, vol. 13, no. 3, pp. 227–286, 1999.

[37] A. R. Karlin and D. Kempe, "Beyond VCG: frugality of truthful mechanisms," *IEEE Symposium on Foundations of Computer Science*, pp. 615–624, Pittsburgh, PA, USA, October 2005.

[38] R. Akcelik, "Efficiency and drag in the power-based model of fuel consumption," *Transportation Research Part B: Methodological*, vol. 23, no. 5, pp. 376–385, 1989.

[39] Highway Capacity Manual, *U.S. Customary Units,* Transp. Res. Board (TRB), Washington, DC, USA, 2000, http://gen.lib.rus.ec/book/index.php?md5=da1d3ae5e4a32e3d858e6650855fb83c.

[40] J. Tan, T. Yang, Y. Zhang, and T. Z. Qiu, "Evaluation of vehicles' platooning on expressways based on V2X," in *Proceedings of the 5th International Conference on Transportation Information and Safety (ICTIS)*, pp. 369–375, Liverpool, LP, UK, July 2019.